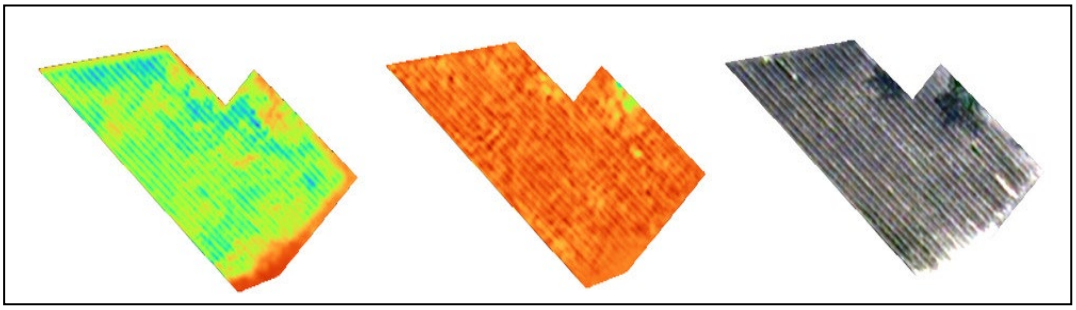
Australian Government
Wine Australia

Government of South Australia
Department of Primary Industries and Regions

THE UNIVERSITY of ADELAIDE

consilium .TECHNOLOGY

Rapid surveillance and assessment of fire damage in South Australian vineyards for decision making



COMBINED FINAL REPORT TO WINE AUSTRALIA

Project number	WA 2003	WA 2004
Principal Investigators	Cassandra Collins	Saisai Ma and Andy Clarke
Research organisation	University of Adelaide	GAIA Innovations Pty Ltd (Consilium Technology)

June 2022 (updated April 2023)

Table of Contents

1. Acknowledgments 3
2. Abstract 4
2. Executive summary 5
3. Background 6
4. Project Aims 8
4.1 Consilium Technology Outputs and Activities 8
4.2 University of Adelaide Outputs and Activities 10
5. Method 11
5.1 Pre-processing of fire damage assessments 11
5.1.1 Conversion of University of Adelaide data into geospatial format 11
5.1.2 Preparation of satellite imagery for modelling 13
5.2 Machine learning models 13
5.2.1 HDBScan 13
5.2.2 Quadratic discriminant analysis 13
5.2.3 XGBoost 14
5.3 Model evaluation 14
5.3.1 Cross validation 14
5.3.2 Metrics 15
5.4 Fire damage recovery assessments 15
5.4.1 Sites and Experimental Design 15
5.4.2 Fire damage assessments 16
5.4.3 Vine Recovery - canopy growth, vine fertility and starch concentration 16
6. Results/Discussion 18
6.1 Analysis of University of Adelaide data 18
6.1.1 Modelling on burn severity from satellite imagery 19
6.1.2 Damage ratio 20
6.1.3 Fire damage assessment comparisons 20
6.1.4 Summary 24
6.2 Analysis of WGCSA data 26
6.2.1 WGCSA data 26
6.2.2 Modelling of burn severity from satellite imagery 31
6.2.3 Damage ratio 39
6.2.4 Summary 39
6.3 Vine recovery after fire damage 41
6.3.1 Canopy Growth 41
6.3.2 Vine fertility and starch concentration 42
6.3.3 Summary 46
7. Outcome/Conclusion 49
8. Recommendations 50
9. Appendix 1: Communication 51
10. Appendix 2: Intellectual Property 52
11. Appendix 3: References 53
12. Appendix 4: Staff 57

1. Acknowledgments

This project team gratefully acknowledge funding contributed by the Government of South Australia through the SA Wine Industry Development Scheme. Funding was also provided by Wine Australia, with levies from Australia's grapegrowers and winemakers and matching funds from the Australian Government.

2. Abstract

In December 2019, a bushfire occurred in the Adelaide Hills, South Australia, where 25,000 hectares were burnt resulting in various degrees of damage. The ability to coordinate and plan recovery after a fire event relies on robust and timely data. The current process to assess damage to vineyards from fire is time consuming, subjective, or semi-quantitative at best. This study compares the rapid assessment and mapping of fire damage using high-resolution satellite imagery with more traditional ground-based measures. Correlations between ground visual fire damage assessments and post-fire NDVI and VARIgreen satellite imagery were significant but ranged from relatively weak to moderate negative correlations. Severely damaged vines had reduced canopy growth, low fertility and low starch concentrations in buds and canes. In contrast, vines that received minor-moderate damage were able to recover within one to two years. Results from this study will allow stakeholders to manage decisions in relation to fire recovery by improving the efficiency and effectiveness of their response.

2. Executive summary

There is increasing scientific consensus that climate change is one of the underlying causes of the prolonged dry and hot conditions that have increased the risk of extreme fire weather in many countries around the world.

In December 2019, a bushfire occurred in the Adelaide Hills, South Australia, burning through 25,000 hectares, including some vineyards. Vineyards and their infrastructure were scorched resulting in damage to varying degrees. The ability to coordinate and plan recovery after a fire event relies on robust and timely data. The current practice for measuring the scale and distribution of fire damage is to walk or drive the vineyard and score individual vines based on visual observation. The process is time consuming, subjective, and semi-quantitative at best. After the December 2019 fires, it took many months to access properties and estimate the area of vineyard damaged. This study compared the rapid assessment and mapping of fire damage using high-resolution satellite imagery with more traditional ground-based measures. Correlations between ground visual fire damage assessments and post-fire NDVI (-0.7 to 0.04) and VARIgreen (-0.333 to 0.074 for only the University of Adelaide trial blocks) satellite imagery were significant but showed no correlation to a moderate or weak negative correlation respectively.

Canopy growth, vine fertility and starch concentrations were tracked in the two seasons following the fire event to assess vine recovery. Canopy health in the seasons following the fires correlated to the severity of the initial fire damage. Severely damaged vines had reduced canopy growth, were infertile or had very low fertility as well as lower starch concentrations in buds and canes during dormancy, which reduced productivity in the seasons following the bushfire event. In contrast, vines that received minor to moderate damage were able to recover within one to two years.

Delays of 3 to 4 months in gathering the ground truth data set, coordinated in a separate project through Wine Grape Council of South Australia (WGCSA), had an impact upon the reliability of this data relative to the imagery captured immediately post-fire event due to regrowth of the vines. This factor, and the relatively small ground truth data sets, limited the ability to create a reliable multi-class variable damage model. However, several models have been created capable of determining a binary value for damage on known vineyard sites across the fire scar, with relative confidence. In the event of future fires this can be deployed immediately, and a coordinated collection of concurrent ground truth data could help form better data sets for improved accuracy and to develop variable damage models. Tools have been developed that rapidly and affordably capture the extent and severity of damage over large vineyard areas to allow producers, government, and industry bodies to make more efficient decisions during the post-fire recovery. The benefits of this will flow to the grower through better fire recovery planning, coordination and delivery, providing more certainty and reducing stress.

We acknowledge the funding support of the Government of South Australia through the SA Wine Industry Development Scheme, WGCSA for access to the ground truth data set, all growers that provided research locations for ongoing testing, and Wine Australia for funding and coordinating the project.

3. Background

Many vineyards around the world are located in regions characterised by persistent hot and dry summers. Warm springs, hot summers, dry vegetation, strong winds and low humidity create the ideal conditions for bushfires (wildfires) (Hantson et al., 2016). While they play an important role in our ecosystems (Lloret et al., 2002), an increase in their occurrence and frequency has been observed in recent years (Westerling et al., 2006; Dutta et al., 2016; Westerling 2016) and climate change has been linked to fire seasons starting earlier and finishing later, resulting in greater geographic coverage and duration, intensity, as well as economic and social impacts (Westerling 2016, Jolly et al., 2015).

Despite the increase in bushfires, there is relatively little research on their impacts on grapevines and studies have largely concentrated on the analysis and/or amelioration of smoke taint in grapes and wine (Kennison et al., 2007; Ristic et al., 2011; Wilkinson et al., 2011; De Vries et al., 2016; Fuentes, et al., 2019; Ristic et al., 2016; van der Hulst et al., 2019; Mirabelli-Montan et al., 2021). However, in some cases, vineyards have been subjected to fire damage and very little is known about their growth and recovery after this occurrence. Hamilton (2020) outlines the practical considerations when assessing fire damage and planning for vineyard recovery. Scarlett et al. (2011) assessed vineyard viability using visual assessments of leaf damage and cordon, trunk, and latent bud tissue viability after the 2009 fires in Victoria, Australia. They concluded that multiple assessment methods were required to rapidly and accurately capture fire damage. A study of vine recovery (Pinot Noir and Semillon) after a bushfire in 2008 in South Australia reported that vines with visual symptoms of fire-damage had lower yields in the following season but made nearly a full recovery by the second season (Collins et al., 2013). Lower yields were attributed to reduced fruitfulness and bunch weight (lower berry numbers per bunch). However, fire damage to this vineyard was isolated to areas on the vineyard boundaries near the surrounding trees. To better understand vine recovery after a fire a greater range in fire damage should be investigated.

One of the challenges with studying fire damage in vineyards is that the intensity of fire can vary considerably across a vineyard or a block of vines, as illustrated in previous articles (Wilkinson and Collins 2010; Scarlett et al., 2011; Collins et al., 2013; Hamilton 2020). The trauma and competing recovery interests following fire events make it difficult for growers, industry bodies and government to rapidly assess the level of damage incurred. This information is critical in developing effective recovery plans in the short and medium terms for all stakeholders.

In December 2019, a bushfire event occurred in the Adelaide Hills, South Australia, where 25,000 hectares were burnt and caused various degrees of scorching and infrastructure damage in vineyards and surrounding areas. The exercise to visually assess (ground truth) damage to 1100 hectares of vineyards following this fire event by walking affected blocks was time consuming, taking months to complete. Additionally, only a small sample of each vineyard was assessed and used to estimate the total damage across each property. Delays in completing the assessment meant that true estimates of initial damage were difficult to accurately calculate as some vines which were initially defoliated produced new foliage in the interim.

Numerous studies suggest the use of satellite data as a more cost-effective tool to assess agricultural damage (De Leeuw et al., 2014; Black et al., 2016; Bokusheva et al., 2016). To overcome the challenge of rapid and accurate assessment after fire damage, satellite imagery may be a good solution, particularly vegetation indices (Cunha et al., 2010; Devaux et al., 2019; Khaliq et al., 2019; Cogato et al., 2020). Normalised Difference Vegetation Index (NDVI) is a commonly used vegetation index which makes use of the red and near infrared bands. It has been used in studies relating to canopy growth and vigour (Xue and Su, 2017) and was found to be the most commonly used vegetation index in viticulture publications (Giovos et al., 2021). VARIgreen (Often referred to as just VARI) was designed to be less sensitive to

atmospheric conditions than NDVI (Gitelson et al., 2002). Although, it was initially developed on corn and wheat crops, it has been used successfully in vineyard studies previously (Cogato et al., 2021; Giovos et al., 2021) and was investigated in this study.

Identifying vineyards on a satellite image has previously required large amounts of human effort to locate and draw within standard GIS systems and is even more difficult without vegetation following a fire event. The GAIA project technology developed by Consilium Technology, which identifies and locates vineyards with machine learning from satellite images, was utilised to determine where vineyards were located within the burn scar. This same technology delivered the 2018, 2019 and 2020 National Vineyard Scans for Wine Australia. Initial ground truth data—collected through a prior project funded through the SA Wine Industry Development Scheme (SAWIDS)—was provided by the South Australian Department of Primary Industries and Regions (PIRSA).

The aims of this study were to:

1. Investigate if satellite imagery can rapidly and objectively map fire damage; and
2. Understand the relationship between fire damage and the long-term viability and productivity of damaged vines.

It was hypothesised that satellite imagery would correlate with ground truth data and that vine recovery would vary depending on the initial fire damage. A gain in knowledge in this area will provide growers with a better understanding of the likely effect of fire damage on vine health and productivity, to improve vineyard management after a bushfire.

4. Project Aims

This project aimed to:

1. Develop a new tool to rapidly, objectively and cost-effectively map fire damage at the block level using high-resolution satellite imagery.
2. Provide growers with a better understanding of the likely effect of fire damage on vine health and productivity, to improve grower knowledge and vineyard management after a bushfire.
3. Understand the relationship between satellite imagery captured after a fire event and the long-term viability and productivity of damaged vines.

The following sections provide a reconciliation of the planned project deliverables against the outputs achieved by both project partners, University of Adelaide and Consilium Technology (Gaia Innovations Pty Ltd).

4.1 Consilium Technology Outputs and Activities

Outputs and activities to achieve project aims are shown below in Tables 4.1.1 and 4.1.2. All outputs and activities were achieved as outlined below.

Table 4.1.1. Outputs and Activities 2020–21

Year 1	Output	Target Date	Activities
A	Satellite imagery access provided to project partners and stakeholders, including Wine Australia, University of Adelaide, Adelaide Hills Regional Association and impacted grape growers (1100 Ha)	30 November 2020	Pre fire imagery and two seasons of satellite imagery offered to all fire affected growers and partners, and provided to registered parties through the GAIA/Green Brain app. Presentation delivered to growers in the Adelaide Hills, September 2020.
B	Validation data set built	30 November 2020	Data from SAWIDS-funded fire assessment project (coordinated by Wine Grape Council of SA) sourced and vetted for incorporation into modelling. This highlighted data misalignment, likely due to time differences between the fire event and when fire damage data was captured.
C	Communicate findings to industry	28 February 2021	Presentation of preliminary results to SA Wine regions at the National Bushfire Conference, May 2021.
D	Initial report on spatial analysis of ground truthed vineyards (i): Comparisons between before and immediately after the fire and grading burn severity.	30 June 2021	Remote sensing spatial assessment of fire damage. Correlations and visual assessment were performed.

Table 4.1.2. Outputs and Activities 2021–22

Year 1	Output	Target Date	Activities
A	Report on spatial analysis of ground truthed vineyards (ii): correlation between remote sensing and Ground measurements such as fruitfulness and canopy recovery.	31 December 2021	Data with GPS coordinates along with University of Adelaide (UoA) burn damage categories was converted into geospatial files. Low number of data points and often low GPS accuracy meant the data was analysed in terms of summary statistics per damage class per field. The lack of the same vines repeatedly measured over time meant no correlation could be performed between the ground based and satellite-based results.
B	Demonstration of new bushfire assessment tool to SA Wine industry.	30 April 2022	Multiple machine learning models (including unsupervised and supervised learning approaches) have been built to work with the existing GAIA model to predict the fire damages and the damage ratio. While the models generated reasonably good results on existing data, more high quality ground truth data is required to improve performance. Findings to be delivered at the Australian Wine Industry Technical Conference in June 2022. Discussions with regional and state bodies to highlight the opportunities in future bushfire events have begun.
C	Increase grower community confidence with Agtech	30 April 2022	Limited uptake and response to surveys at the beginning of the project made it difficult to compare changes in grower sentiment to AgTech.
D	Final report to Wine Australia	30 June 2022	Final report delivered. A series of models has increased our ability to identify fire damaged vineyards. With a limited data set, and without pre-fire data, we were unable to predict recovery of individual vines. The lack of confidence in the fire damage class labels provided (due to time delays), makes it difficult to assess vine recovery.

4.2 University of Adelaide Outputs and Activities

Outputs and activities to achieve project aims are shown below in Tables 4.2.1 and 4.2.2. All outputs and activities were achieved as outlined below.

Table 4.2.1. Outputs and Activities 2020–21

Year 1	Output	Target Date	Activities
A	Fire damaged sites identified	31 July 2020	Fire-damaged sites identified and visually rate fire damage to allow monitoring of vineyard recovery and validation of imagery captured.
B	Validation data set for 2020	31 December 2020	Evaluation of the health and productivity of burnt vines using performance assessments, vitality stains, bud fertility and carbohydrate analysis performed at different developmental stages.
C	Communicate findings to industry	28 February 2021	Presentation of results to SA wine regions.

Table 4.2.2. Outputs and Activities 2021–22

Year 2	Output	Target Date	Activities
A	Validation data set for 2021	31 December 2021	Evaluation of the health and productivity of burnt vines using performance assessments, vitality stains, bud fertility and carbohydrate analysis performed at different developmental stages.
B	Communicate findings to industry	28 February 2022	Presentation of results to SA wine regions.
C	Final report to Wine Australia	30 June 2022	Prepare final report comparing validation data and imagery captured. Recommendations for bushfire recovery management presented.

5. Method

5.1 Pre-processing of fire damage assessments

5.1.1 Conversion of University of Adelaide data into geospatial format

Data was supplied by researchers at the University of Adelaide (UoA) to Consilium Technology via an online storage system. A handover meeting was held to explain the data and its collection. Follow up emails and conversations have been welcomed where questions have arisen.

The data supplied by UoA can be broken down into four broad categories: canopy growth, bud fertility, harvest data and fire damage across nine vineyard blocks. Not all data is available for every vineyard block and not all data is of a format suited to geospatial conversion. Table 5.1.1 summarises the data types received and their suitability for conversion to a geospatial format.

Table 5.1.1. Summary of data types received

Data Type	Brief Description	Suitable for Conversion to Geospatial Format
Canopy Growth		
Canopy Growth	Single Excel document per vineyard block. Spreadsheet per date of sampling. Plant Area Index (PAI) and Porosity recorded along with GPS location.	Yes
Bud Fertility		
Bud Dissections 2020 and 2021	Separate Excel documents provided for 2020 and 2021. Spreadsheet per vineyard block. Bud dissection results given by Cane Number. No GPS coordinates.	Not at this point. Although potential to link information via Cane Number to Block and Zone Level Data.
IP Measurements 2020 & 2021	Separate Excel documents provided for 2020 and 2021. Spreadsheet per vineyard block. IP measurement results given by Cane Number. No GPS coordinates.	Not at this point. Although potential to link information via Cane Number to Block and Zone Level Data.
Block Level IP No and Area 2020 & 2021	Single Excel document containing a spreadsheet for each vineyard block. IP number and Area given per Cane Number. GPS coordinates included.	Yes
Zone Level IP No and Area 2020 & 2021	Single Excel document containing a spreadsheet for each vineyard block. IP No and Area given per Cane Number and replicate. Fire damage zone also indicated. GPS coordinates included.	Yes
Harvest Data		
2021 Bunch Counts	Single Excel document containing a spreadsheet for each vineyard block. Bunch numbers per m based on section and replicates. No GPS coordinates or other linking information.	No
2021 Bunch Data	Single Excel document containing a spreadsheet for each vineyard block. Various attributes recorded for each bunch by section and replicate. No GPS coordinates or other linking information.	Not at this point. Although potential to link information via Cane Number to Block and Zone Level Data.
Fire Damage		
Block Assessments after Fire	Single Excel document containing a spreadsheet for each vineyard block. Fire damage classification given for each row and vine of the vineyard block. No GPS coordinates.	Yes

Based on Table 5.1.1, data identified as suitable for conversion were processed in geospatial format. The procedure varies by data type and the steps taken are outlined in the previous report (see Appendix A).

5.1.2 Preparation of satellite imagery for modelling

The pre-fire satellite imagery for all blocks was taken on 18 December 2019, while most post-fire satellite imagery was taken just after bushfire, but two of them were taken three months later. Ground truthing was performed 4-5 months after the fire (see Table 3).

The satellite imagery procured was both orthorectified and atmospherically corrected by the provider (MAXAR) through their GBDX platform and supplied as reflectance. The imagery was then pansharpened to the delivered panchromatic image resolutions.

Georeferencing is performed using the QGIS Georeferencer tool and requires the selection of ground control points (GCPs). GCPs are points which can be accurately identified in both the base image and the image to be georeferenced. Following georeferencing, all satellite images are resampled to 50cm (to match the lowest resolution) to ensure consistency across the dataset.

Due to the varying resolutions, all imagery for which there was complete vine by vine fire damage was resampled to 0.5m post georeferencing. This was done using bilinear resampling. While not ideal to lose resolution across many of the images, for the purposes of the models that were planned for consideration, it was necessary for all the images to be of the same resolution. This was done after georeferencing in order to minimise the effects of the downsampling on georeferencing.

5.2 Machine learning models

5.2.1 HDBScan

The unsupervised learning algorithm, HDBScan, has been utilised to identify damaged and undamaged vines. HDBScan is a clustering algorithm which extends DBScan by converting it into a hierarchical clustering algorithm, and then using a technique to extract a flat clustering based in the stability of clusters. Performs DBSCAN over varying epsilon values and integrates the result to find a clustering that gives the best stability over epsilon. This allows HDBSCAN to find clusters of varying densities (unlike DBSCAN), and be more robust to parameter selection.

In practice this means that HDBSCAN returns a good clustering straight away with little or no parameter tuning -- and the primary parameter, minimum cluster size, is intuitive and easy to select.

5.2.2 Quadratic discriminant analysis

This operator performs a quadratic discriminant analysis (QDA). QDA is closely related to linear discriminant analysis (LDA), where it is assumed that the measurements are normally distributed. Unlike LDA however, in QDA there is no assumption that the covariance of each of the classes is identical. To estimate the parameters required in quadratic discrimination more computation and data is required than in the case of linear discrimination. If there is not a great difference in the group covariance matrices, then the latter will perform as well as quadratic discrimination. Quadratic Discrimination is the general form of Bayesian discrimination.

Discriminant analysis is used to determine which variables discriminate between two or more naturally occurring groups. For example, an educational researcher may want to investigate

which variables discriminate between high school graduates who decide (1) to go to college, (2) NOT to go to college. For that purpose the researcher could collect data on numerous variables prior to students' graduation. After graduation, most students will naturally fall into one of the two categories. Discriminant Analysis could then be used to determine which variable(s) are the best predictors of students' subsequent educational choice. Computationally, discriminant function analysis is very similar to analysis of variance (ANOVA). For example, suppose the same student graduation scenario. We could have measured students' stated intention to continue on to college one year prior to graduation. If the means for the two groups (those who actually went to college and those who did not) are different, then we can say that the intention to attend college as stated one year prior to graduation allows us to discriminate between those who are and are not college bound (and this information may be used by career counsellors to provide the appropriate guidance to the respective students). The basic idea underlying discriminant analysis is to determine whether groups differ with regard to the mean of a variable, and then to use that variable to predict group membership (e.g. of new cases).

Discriminant Analysis may be used for two objectives: either we want to assess the adequacy of classification, given the group memberships of the objects under study; or we wish to assign objects to one of a number of (known) groups of objects. Discriminant Analysis may thus have a descriptive or a predictive objective. In both cases, some group assignments must be known before carrying out the Discriminant Analysis. Such group assignments, or labeling, may be arrived at in any way. Hence Discriminant Analysis can be employed as a useful complement to Cluster Analysis (in order to judge the results of the latter) or Principal Components Analysis.

5.2.3 XGBoost

XGBoost is a decision-tree-based ensemble Machine Learning algorithm that uses a gradient boosting framework. In prediction problems involving unstructured data (images, text, etc.) artificial neural networks tend to outperform all other algorithms or frameworks. However, when it comes to small-to-medium structured/tabular data, decision tree based algorithms are considered best-in-class right now. Since its introduction, XGBoost has not only been credited with winning numerous Kaggle competitions but also for being the driving force under the hood for several cutting-edge industry applications.

5.3 Model evaluation

5.3.1 Cross validation

Cross-validation is a resampling method that uses different portions of the data to test and train a model on different iterations. It is mainly used in settings where the goal is prediction, and one wants to estimate how accurately a predictive model will perform in practice. In a prediction problem, a model is usually given a dataset of known data on which training is run (training dataset), and a dataset of unknown data (or first seen data) against which the model is tested (called the validation dataset or testing set). The goal of cross-validation is to test the model's ability to predict new data that was not used in estimating it, in order to flag problems like overfitting or selection bias and to give an insight on how the model will generalize to an independent dataset (i.e., an unknown dataset, for instance from a real problem).

In k-fold cross-validation, the original sample is randomly partitioned into k equal sized subsamples. Of the k subsamples, a single subsample is retained as the validation data for testing the model, and the remaining k − 1 subsamples are used as training data. The cross-validation process is then repeated k times, with each of the k subsamples used exactly once as the validation data. The k results can then be averaged to produce a single estimation. The advantage of this method over repeated random sub-sampling (see below) is that all observations are used for both training and validation, and each observation is used for

validation exactly once. 10-fold cross-validation is commonly used, but in general k remains an unfixed parameter.

The Leave-One-Out Cross-Validation, or LOOCV, procedure is used to estimate the performance of machine learning algorithms when they are used to make predictions on data not used to train the model. It is a computationally expensive procedure to perform, although it results in a reliable and unbiased estimate of model performance. Although simple to use and no configuration to specify, there are times when the procedure should not be used, such as when you have a very large dataset or a computationally expensive model to evaluate.

5.3.2 Metrics

To evaluate the model performance, we compare predictions of machine learning models with the ground truth, using the metrics of F1-score. The F1-score is a classical measure of a test's accuracy. It is calculated from the precision and recall of the test, where the precision is the number of true positive results divided by the number of all positive results, including those not identified correctly, and the recall is the number of true positive results divided by the number of all samples that should have been identified as positive. Precision is also known as positive predictive value, and recall is also known as sensitivity in diagnostic binary classification. For the calculation of precision, recall and the F1-score.

Note that the number of F1-score discussed in the following sections is the weighted average F1-score. We calculated the F1-score for each individual class (e.g. undamaged and damaged), then used the sample sizes of classes as the weights to obtain the final weighted average F1-score.

5.4 Fire damage recovery assessments

5.4.1 Sites and Experimental Design

Ten vineyard sites across the Adelaide Hills region that were damaged in the fire were selected for this study. Selection of sites was based on the owners' willingness to participate and varying degrees of fire damage across the block. These vineyards were assessed for initial fire damage and vine recovery was monitored over a period of two years from February 2020 to March 2022. Details on the vineyard sites selected in the study are shown in Table 5.4.1.

Table 5.4.1. Site details of selected vineyards for the assessment of initial fire damage and vine recovery.

Site Details	Variety	Block Size (Ha)	Pruning Method	Visual ground assessment of damage
A	Pinot Gris	1.1	Spur	All vines assessed and three zones of fire damage
B	Sauvignon Blanc	2.1	Cane	All vines assessed and three zones of fire damage
C	Chardonnay	1.4	Cane	All vines assessed and three zones of fire damage
D	Sauvignon Blanc	0.7	Cane	All vines assessed and three zones of fire damage
E	Sauvignon Blanc	0.7	Cane	All vines assessed and three zones of fire damage
F	Pinot Noir	1	Spur	Three zones of fire damage*
G	Pinot Noir	1.1	Spur	Three zones of fire damage
H	Chardonnay	8.8	Spur	All vines assessed and three zones of fire damage
I	Pinot Noir	0.8	Spur	Three zones of fire damage
J	Pinot Noir	1.4	Spur	Three zones of fire damage

*Three zones of 12 vines per zone, classified as severe, minor-moderate and no visible damage were selected for detailed assessment.

5.4.2 Fire damage assessments

Visual ground assessments of fire damage were made in February/March 2020 for Blocks A-E and for Blocks F-J in early April 2020. As these assessments were made 2-4 months after the fire it was difficult to separate minor and moderate fire damage due to some shoot regrowth. As such, three classifications were used to categorise fire damage: severe, minor-moderate and no visible damage. Ground visual assessments were carried out on every vine at six of the ten sites after the fire event (Sites A-E and J). Due to the resources available for the research study it was not possible to undertake assessments of every vine, at every site for all measurements. Therefore, three damage zones (12 vines per damage zone) at all ten sites were selected and represented the three categories of damage; severe, minor-moderate and no visible damage.

5.4.3 Vine Recovery - canopy growth, vine fertility and starch concentration

To assess vine recovery in the seasons following the fire event, canopy growth, vine fertility and starch concentration of bud and cane tissues were assessed in the 2020/21 and 2021/22 growing seasons.

The VitiCanopy app was used to capture upward looking images of grapevine canopies and calculate Plant Area Index (PAI) using the method described in De Bei *et al*., (2016). Canopy assessments were made at each site at 3-5 time points (COVID-19 restrictions limited access at some sites) during the 2020/2021 growing season and 5 time points in the 2021/2022 growing season. Due to the level of fire damage and productivity of the vineyard area, owners made the decision to remove vines at site G in 2020/21 and sites I and J in 2021/22. As such, measures were not recorded for these sites after vine removal. Assessments were made at each of the selected zones of damage (severe, minor-moderate and no visible damage) to monitor canopy growth over time.

Vine fertility was evaluated at two developmental stages over two seasons following the fire event; winter dormancy via bud dissection analysis to assess bud fertility and at harvest via the assessment of yield components.

Bud fertility assessments were made on canes collected from all sites; 30 canes per fire damage zone. Compound buds at node positions 1-4 at spur pruned sites and node positions 1-10 at cane pruned sites were dissected using a razor blade to make transverse cuts through the bud axes as described in Rawnsley and Collins, 2005. The bud was then observed under a light microscope (Model EZ4W, Leica, Heerbrugg, Switzerland) at 25x magnification. The number of inflorescence primordia (IP) in the primary bud of each compound bud was recorded. If the primary bud was necrotic, the largest secondary bud was assessed instead (assumption that secondary bud would compensate for the loss of the primary bud). Images of dissections were taken using the Leica AirLab App, and the cross-sectional area of IP (IA) was measured on the images using software Image J (NIH, USA).

Yield components—bunch number per shoot, bunch weight, berry number per bunch and berry weight—were measured at harvest on 12 vines from each fire damage zone at each site in growing seasons 2020/21 and 2021/2022 (except where vineyards were removed or reworked).

During winter dormancy, samples of canes and buds were collected from vines at each site from each of the fire damage zones in both the 2020/21 and 2021/2022 growing seasons. All samples were kept on dry ice until storage in a -80°C freezer and then freeze dried (Alpha 2-4 LSC; John Morris Scientific, Adelaide, Australia). For starch analysis, bud and cane samples were ground in an electrical mill (Model A11, IKA, Germany). Starch analysis was performed using a commercial enzyme assay kit (Total starch assay kit, Megazyme, Ireland) following the method described in Edwards et al. (2011). Using a spectrophotometer (Multiskan Spectrum, model 00300011, Thermo Electron Corporation, Vantaa, Finland) the absorbance was read at 505 nm and the starch content determined using a glucose standard curve.

Fire damage comparisons, seasonal effects and the interaction of the two (fire damage x season) were analysed via two-way ANOVA; means were then separated using the Tukey's test. Where vines were removed after the first season and for PAI assessments, a one-way ANOVA was performed. XLSTAT® (Version 2022.1.1 Premium 1248, Addinsoft SARL, Paris, France) was used for all statistical analyses. Means were separated at a significance level of $p < 0.05$ for all data.

6. Results/Discussion

6.1 Analysis of University of Adelaide data

In Consilium Technology (CT) data, there are five classes (Undamaged, Minor Damage, Moderate Damage, Severe Damage and No Growth) labelled in the ground truthing, while UoA data only used four different classes (Undamaged, Damaged, Severely Damaged to Dead, and Missing) for the labelling. To make them consistent, labels in UoA data have been also converted into binary and 3 classes, see Table 6.1.1.

Table 6.1.1. Additional adopted UoA fire damage classification schemes.

Label	Classification	Old Classes
3 Class Classification		
0	Undamaged	Undamaged
1	Moderate Damage	Damaged
2	Severe Damage	Severely Damaged to Dead, and Missing
Binary Classification		
0	Undamaged	Undamaged
1	Damaged	Damaged, Severely Damaged to Dead, and Missing

The data is pre-processed for machine learning modelling by extracting the same points used for the NDVI correlation analysis. That is all pixels in a 1.5x1.8m buffer of each sampled vine. Each of these pixels is assigned a fire damage class from the fire damage raster image. Figures 6.1.1 and 6.1.2 show the distributions of 2-class and 3-class data.

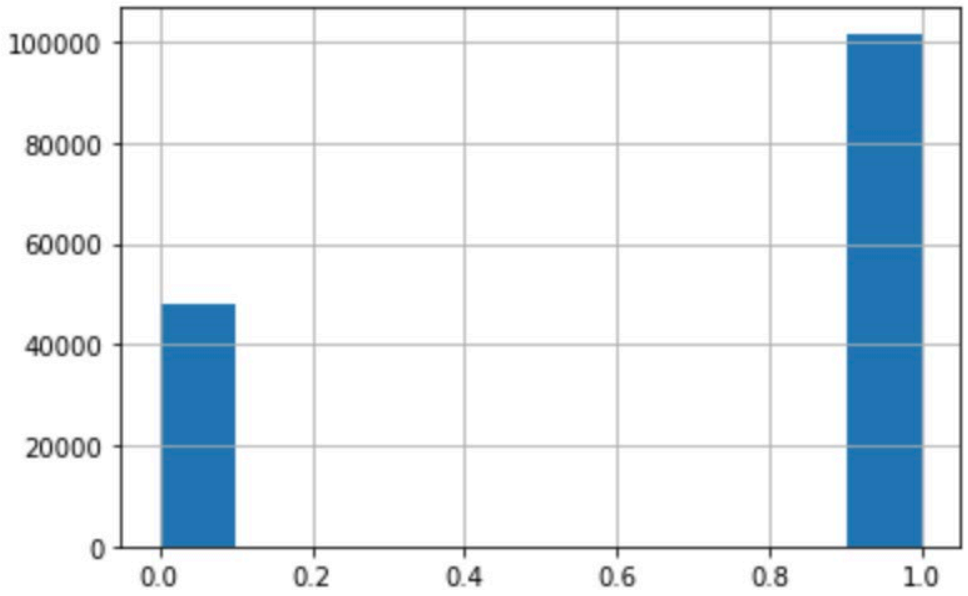


Figure 6.1.1. The distribution of 2 classes UoA data, Class 0: Undamaged and Class 1: Damaged.

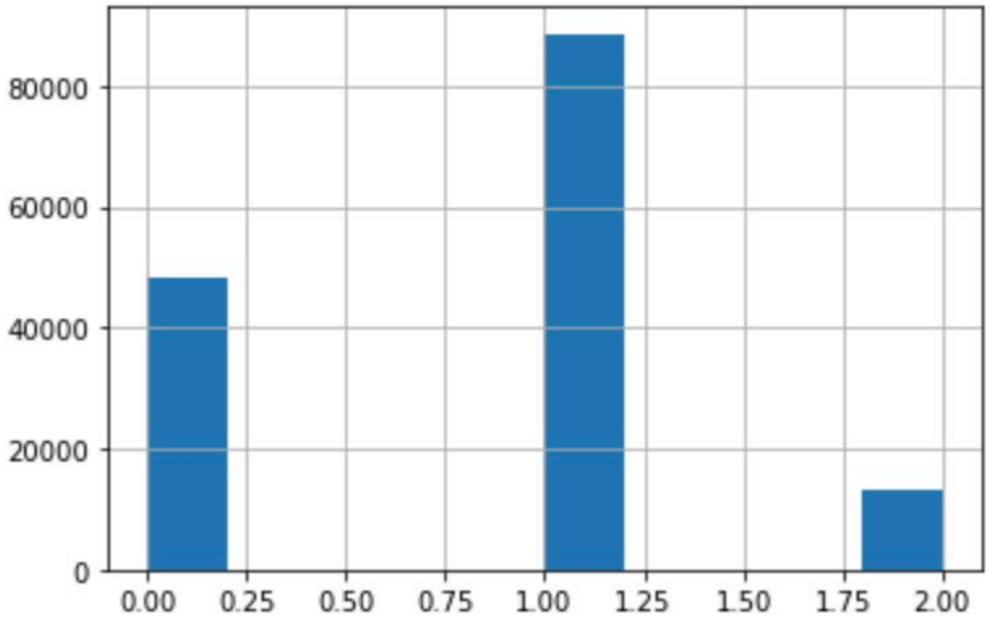


Figure 6.1.2. The distribution of 3 classes UoA data, Class 0: Undamaged, Class 1: Moderate Damaged and Class 2: Severe Damaged.

6.1.1 Modelling on burn severity from satellite imagery

A popular and efficient machine learning model, XGBoost, has been applied to makes predictions on UoA data. 10-fold cross validation and leave-one-out cross validation were employed to evaluate the model performance.

Table 6.1.2. F1-score for XGBoost (cross validation) for each vineyard block for 3 and 2 class models. Note that F1-score here indicates a weighted average F1-score on all classes.

Models	Data	Average F1-Score
3 Class Model	Training	0.58
	Testing	0.57
Binary Model	Training	0.70
	Testing	0.68

Table 6.1.3. F1-score for XGBoost (leave one out cross validation) for each vineyard block for 3 and 2 class models. Note that F1-score here indicates a weighted average F1-score on all classes.

Models	Test	Train	F1-Score	Average
3 Class Model	UoA-1	Others	0.46	0.49
	UoA-2	Others	0.55	
	UoA-9	Others	0.21	
	UoA-10	Others	0.74	
Binary Model	UoA-1	Others	0.54	0.62
	UoA-2	Others	0.65	
	UoA-9	Others	0.44	
	UoA-10	Others	0.84	

Tables 6.1.2 and 6.1.3 show the results predicted by XGBoost with 10-fold cross validation and train-test-split. Due to the small data size, the machine learning model does not perform very well. More high-quality data is required to improve the prediction performance.

6.1.2 Damage ratio

Table 6.1.4 shows the comparison of damage ratio between actual and predicted damages, and the corresponding absolute error. We can see that the model cannot precisely predict the damage ratio in most UoA blocks, and the mean absolute error is more than 20%.

Table 6.1.4. Damage ratio for XGBoost for each vineyard block.

Vineyard Block	Damage Ratio		
	Actual	Predicted	Absolute Error
UoA-1	66.42%	97.27%	30.85%
UoA-2	74.16%	60.77%	13.39%
UoA-9	44.90%	3.70%	41.20%
UoA-10	89.20%	97.42%	**8.22%**
Average	-	-	23.42%

6.1.3 Fire damage assessment comparisons

The percentage damage based on ground visual assessments is presented in Table 6.1.5. To spatially visualise the fire damage at the ten sites, pre- and post- fire satellite imagery was generated with ground truth sampling raster and pre- and post- fire NDVI and VARIgreen imagery, and is presented in Figures 6.1.3 and 6.1.4 and Figure 6.1.5 (no ground truth data at block level).

The greatest vine damage due to fire was observed at site J which can be seen when comparing pre- and post-fire satellite imagery and ground truth assessments (Figure 6.1.4, Table 6.1.5) where over 75% of the vineyard displayed visible signs of damage. Sites D and E were scored as having over 80% and 89% damage respectively but most of this was minor to moderate fire damage. At sites A-C the three classifications of fire damage are better represented. A greater proportion of vines assessed as having no visible signs of damage;

26%, 33% and 55% respectively and a higher proportion of severely damaged vines compared to other sites; 9%, 6% and 14% respectively (Table 6.1.5).

Post-fire satellite imagery, ground truth sampling raster and NDVI and VARIgreen imagery sites A-C are similar (Figure 6.1.3), although relatively weak, the correlations presented in Table 6.1.6 support this observation. The negative correlation is expected as increasing fire damage should result in a lower NDVI and VARIgreen, as these increase in value with better plant health. The opposite was observed for sites D, E and J (Figure 6.1.4) where post-fire NDVI and VARIgreen imagery did not correlate well with ground truth assessments (Table 6.1.6). Pre- and post-fire damage differences can be seen between sites F-I but as no site level ground assessments were made due to vineyard access it was not possible to perform correlations.

Table 6.1.5. Fire damage assessments at vineyard block level.

Site	Fire Damage Class	% Damage
A	No visible damage	25.93
	Minor to moderate damage	65.23
	Severe damage	8.84
	Missing vines	0
B	No visible damage	33.43
	Minor to moderate damage	60.96
	Severe damage	5.49
	Missing vines	0.12
C	No visible damage	55.18
	Minor to moderate damage	30.48
	Severe damage	13.98
	Missing vines	0.37
D	No visible damage	18.26
	Minor to moderate damage	78.33
	Severe damage	1.96
	Missing vines	1.45
E	No visible damage	2.78
	Minor to moderate damage	85.78
	Severely damage	3.72
	Missing vines	7.72
J	No visible damage	0
	Minor to moderate damage	51.83
	Severely damage	25.3
	Missing vines	22.87

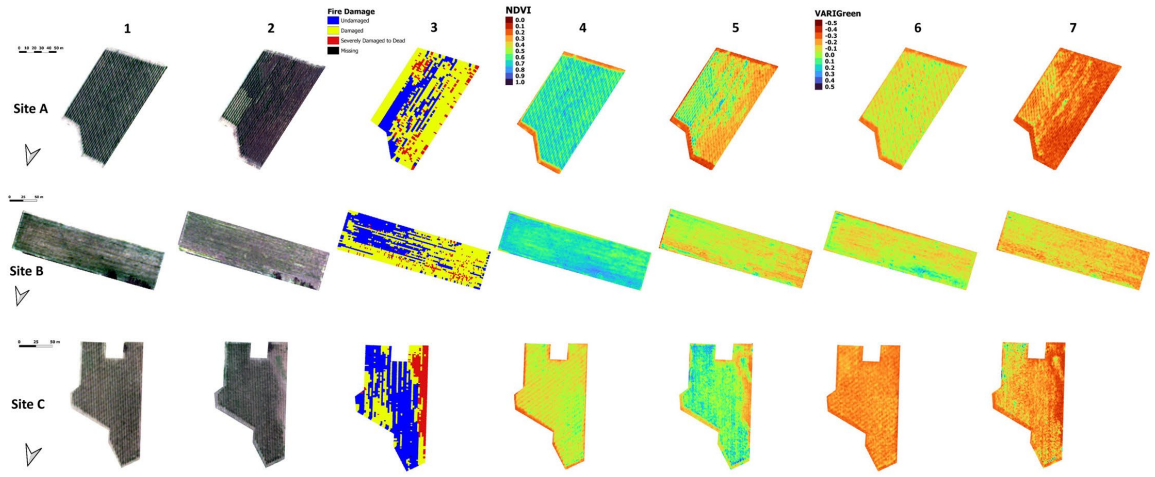


Figure 6.1.3. Pre- and post- fire satellite imagery (1,2), ground truth sampling raster (3), pre- and post- fire Normalised Difference Vegetation Index (NDVI) imagery (4,5) and Visible Atmospherically Resistant Index Green (VARIgreen) imagery (6,7) of sites A, B and C, Adelaide Hills, South Australia. The ground truthing colours are red, yellow and blue to indicate severe, minor-moderate damage and no visible damage; black indicates missing vines.

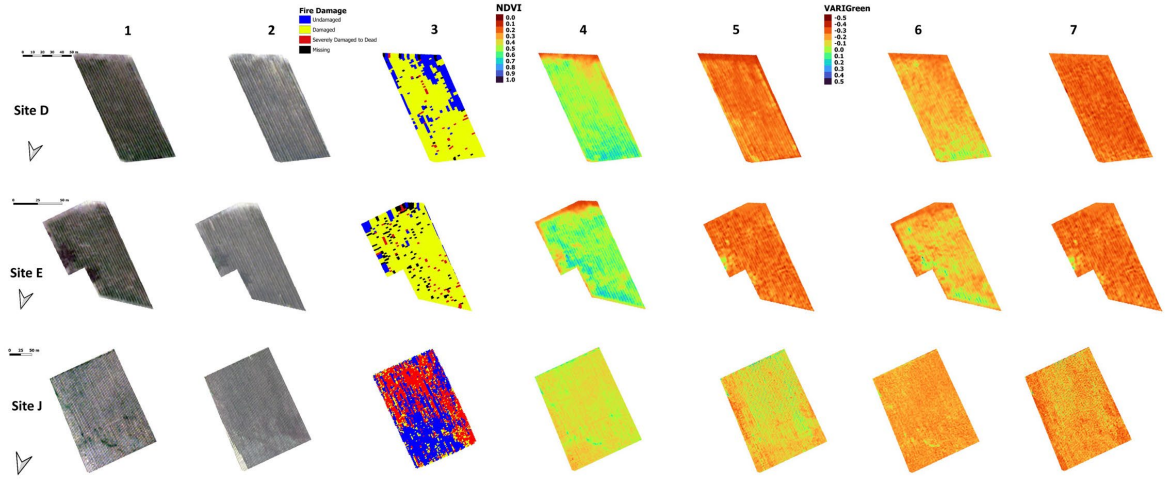


Figure 6.1.4. Pre- and post- fire satellite imagery (1,2), ground truth sampling raster (3), pre- and post- fire Normalised Difference Vegetation Index (NDVI) imagery (4,5) and Visible Atmospherically Resistant Index Green (VARIgreen) imagery (6,7) of sites D, E and J, Adelaide Hills, South Australia. The ground truthing colours are red, yellow and blue to indicate severe, minor-moderate damage and no visible damage; black indicates missing vines.

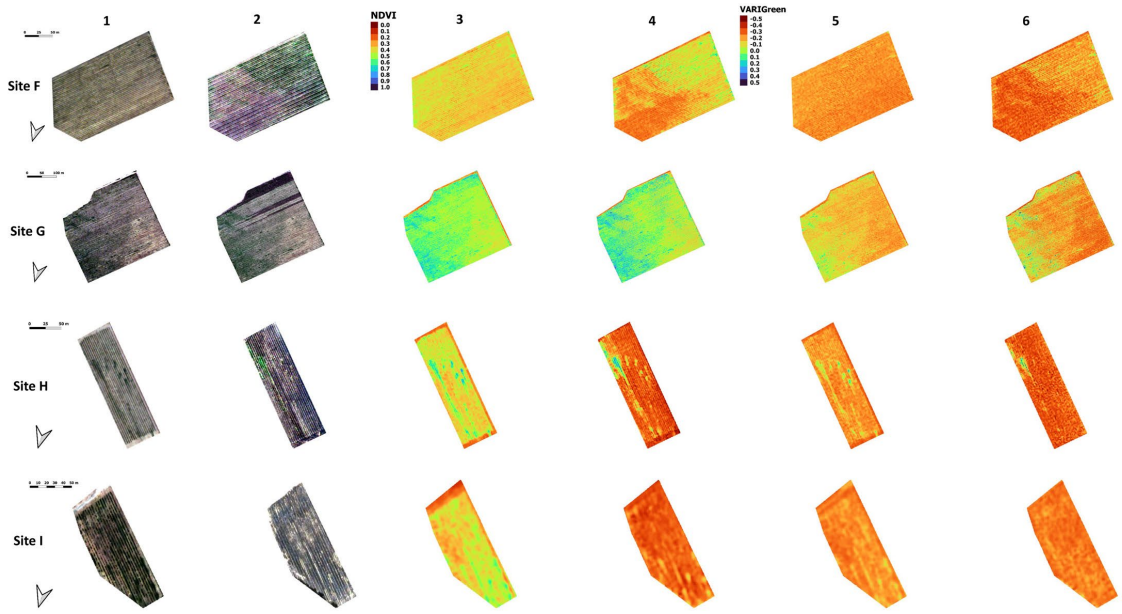


Figure 6.1.5. Pre- and post- fire satellite imagery (1,2), pre- and post- fire Normalised Difference Vegetation Index (NDVI) imagery (3,4) and Visible Atmospherically Resistant Index Green (VARIgreen) imagery (5,6) of sites F, G, H and I, Adelaide Hills, South Australia.

Table 6.1.6. Spearman's Rank coefficients of correlations between ground fire damage assessments NDVI and VARIgreen indices.

Site	Ground assessment and NDVI* correlation	p-value	Ground assessment and VARIgreen* correlation	p-value
A	-0.334	<0.0001	-0.305	<0.0001
B	-0.338	<0.0001	-0.333	<0.0001
C	-0.347	<0.0001	-0.074	<0.0001
D	-0.119	<0.0001	-0.082	<0.0001
E	-0.114	<0.0001	0.077	<0.0001
J	-0.084	<0.0001	-0.307	<0.0001

NDVI - Normalised Difference Vegetation Index and VARIgreen - Visible Atmospherically Resistant Index Green

In order to be able to make decisions regarding how best to manage vines after fire exposure, it is important to understand the effects on the long-term viability of exposed vines. The first step to this process is to appreciate that fire exposure can vary significantly between vineyards due to the fire intensity and exposure time to the fire itself or the radiant heat (Scarlett *et al.,* 2011). This is obviously difficult to assess as it is happening and we tend to assess after the fire event has stopped and when it is safe to enter the vineyard. The next step is to assess the level of damage that has occurred not only to the vines but also to the infrastructure (e.g., trellis and irrigation system) to calculate the damage and prioritise management activities going forward (Hamilton 2020). Typically, the severity of vine damage is classified into groups and based on a visual assessment (Whiting 2012; Scarlett *et al.,* 2011, Hamilton 2020). In this study, three categories were chosen and described as 'no visible damage', 'minor-moderate' and 'severe' damage. No more than three categories were chosen as it was very difficult to separate minor and moderate damage between vines, as there was relatively large variation between vines within these categories, which has also been reported by Scarlett *et al.* (2011) and Hamilton (2020). Without conducting viability assessments on every vine it was also difficult to separate severely damaged vines and those that were dead so for this study they

were grouped together in initial assessments. Variation in damage can be due to a number of reasons such as partial burns to vines, where the fire only burns one side of the vine as it moves through the vineyard, fire intensity differences due to different vineyard floor management such as vegetation and mulches, proximity to surrounding trees and types of surrounding vegetation (Whiting 2012).

Within the ten sites chosen for this study there was a range of different levels of fire damage. Damage ranged from very little at site H to high levels of damage at site J (Figures 6.1.3 - 6.1.5 and Table 6.1.5). The satellite imagery captured and presented in this study demonstrates these differences are more obvious at some sites compared to others. Pre- and post- satellite fire imagery at sites A-C, H and J showed clearer patterns of fire damage compared to sites D-G, and I. When comparing the coefficients of correlations between ground truth data and vegetation indices, A-C and H showed greater correlation with ground data, although still relatively weak. NDVI is the standard baseline vegetation index (Giovos *et al.,* 2021), however, it only uses the red and near infrared bands. While VARIgreen combines information from more bands (red, green and blue) and was included to investigate if coefficients of correlation improved with the inclusion of more bands. It is important to note that these correlations are only indicators of a relationship for these very specific indices and are not indicative of the results that would be expected from a machine learning model trained on all of the bands. As such, a model may find different combinations of bands and/or indices that provide more optimal information regarding the damage state. This will be explored and the focus of future work, following similar strategies as those reported on vineyards affected by frost (Cogato *et al.,* 2020; Li *et al.,* 2021).

6.1.4 Summary

A couple of different strategies were employed to make predictions on UoA data. However, none of them generated good results which may be due to one of the following reasons:

- Ground truth issue. The location of vines was captured vine-by-vine in an Excel spreadsheet. During the pre-processing, the vines were assumed to be evenly spaced along the vine rows, which may misalign the ground truth to images.
- The amount of data. The amount of data is relatively small. More data will definitely help to build a better model.
- Data distribution. The patterns extracted from different blocks may not be consistent, which makes it difficult to be predicted.

Table 6.1.7. Summary of scenarios applied to UoA data.

Scenario	Verdict
Supervised learning - XGBoost Using the model well-trained on CT data for the predictions	The model achieved very good results on CT testing data, so it may be applied to UoA data. The average F1 score is 0.62 and 0.19 on binary and 3 class data respectively. Results are not good. It means that CT and UoA data may not have consistent data distributions. Further investigation is required to test the connection between two data sources.
Supervised learning - XGBoost Classifying pixels in a 1.5x1.8m buffer of each sampled vine 10-fold Cross validation on all samples	The average F1 score is 0.68 and 0.57 on binary and 3 class data respectively. Visual comparison between predictions and the ground truth has been performed. It shows that the model did not perform well to predict the damages.
Supervised learning - XGBoost Classifying pixels in a 1.5x1.8m buffer of each sampled vine Leave one out cross validation on all samples	The average F1 score is 0.62 and 0.49 on binary and 3 class data respectively. Leave one out cross validation allows us to maximise the data used to train the model and repeatedly fit on slightly different data sets. It is a common practice for smaller data sets to minimise the bias. Unfortunately, no significant improvement in results was observed.
Damage ratio Utilising trained XGBoost model to predict damage ratio	The mean absolute error of predicting damage ratio is 23.42%. The model performs poorly at predicting damage ratio.

6.2 Analysis of WGCSA data

6.2.1 WGCSA data

The 'WGCSA data' refers to a collection of visual ratings of fire damage to individual grapevines following the 2019/20 bushfires in the Adelaide Hills of South Australia. The data was collected for a project coordinated by the Wine Grape Council of South Australia (WGCSA) and funded by PIRSA. Further information on the project methods can be found here:
https://www.youtube.com/watch?v=b50XhuZPdZ0&feature=youtu.be

The purpose of accessing the WGCSA data was to determine if it could be used as a ground-truth data set against the satellite imagery.

Table 6.2.1 below shows the dates of both the satellite imagery and the ground truth collection dates.

Table 6.2.1. Satellite imagery date and ground truthing date.

Vineyard Block	Image Date - Pre-fire	Image Date - Post-fire	Ground Truthing Date
CT-1	2019-12-18	2019-12-28	2020-05-04
CT-2	2019-12-18	2019-12-28	2020-04-06
CT-3	2019-12-18	2019-12-28	2020-04-14
CT-4	2019-12-18	2019-12-28	2020-04-06
CT-5	2019-12-18	2019-12-28	2020-04-14
CT-6	2019-12-18	2019-12-28	2020-04-15
CT-7	2019-12-18	2019-12-28	2020-04-27
CT-8	2019-12-18	2019-12-28	2020-05-04
CT-9	2019-12-18	2019-12-28	2020-05-04
CT-10	2019-12-18	2020-03-11	2020-04-21
CT-11	2019-12-18	2020-03-11	2020-04-21
CT-12	2019-12-18	2019-12-25	2020-04-16
CT-13	2019-12-18	2019-12-28	2020-04-16
CT-14	2019-12-18	2019-12-25	2020-04-16
CT-15	2019-12-18	2019-12-28	2020-03-27
CT-16	2019-12-18	2019-12-28	2020-04-02
CT-17	2019-12-18	2019-12-28	2020-04-02
CT-18	2019-12-18	2019-12-28	2020-04-02

CT-19	2019-12-18	2019-12-28	2020-03-26
CT-20	2019-12-18	2019-12-28	2020-04-17
CT-21	2019-12-18	2019-12-28	2020-04-27
CT-22	2019-12-18	2019-12-28	2020-04-08
CT-23	2019-12-18	2019-12-28	2020-04-08

As a starting point for the data analysis, a summary table (Table 6.2.2) was drawn up to indicate the number of sample points (vines) in each vineyard block and the percentage of points from each vineyard block which fall into each of the fire damage classes (see Table 6.2.1).

Table 6.2.2. Number of sample points and percentage of fire damage point data per class for each vineyard block.

Vineyard Block	Number of sample points	Undamaged (%)	Minor Damage (%)	Moderate Damage (%)	Severe Damage (%)	No Growth (%)
CT-1	4153	0	0.1	43	41.27	15.63
CT-2	8177	19.18	50.54	24.41	4.78	1.09
CT-3	6176	0	74.21	22.33	2.59	0.87
CT-4	4433	0.05	51.52	39.27	3.99	5.17
CT-5	5109	0	41.20	25.31	12.45	21.04
CT-6	7573	0	47.33	12.04	5.14	35.49
CT-7	11357	0	5.71	59.11	8.98	26.20
CT-8	5340	0	0.11	79.48	15.43	4.98
CT-9	7099	0	50.71	34.99	6.10	8.20
CT-10	1193	0	0	67.06	28.92	4.02
CT-11	2670	0	0.04	54.61	20.41	24.94
CT-12	1888	0	74.47	25.48	0.05	0
CT-13	877	1.37	48.46	31.81	5.25	13.11
CT-14	3076	0	81.53	16.97	1.40	0.10
CT-15	2416	0	21.65	23.43	23.67	31.25
CT-16	2365	0	26.00	25.92	8.41	39.66
CT-17	6140	0	32.30	16.84	6.69	41.17

CT-18	1236	65.78	12.62	20.63	2.18	1.21
CT-19	9049	7.54	29.63	47.89	5.60	9.34
CT-20	9521	0	74.97	23.20	1.09	0.74
CT-21	1403	47.26	24.09	18.03	2.71	0.08
CT-22	2517	2.19	61.50	24.12	8.14	4.05
CT-23	2458	46.62	30.35	11.64	9.85	1.55

The time lag between the dates for the post-fire satellite imagery and ground truthing (see Table 6.2.2) makes it very challenging to evaluate the performance of machine learning models. This can impact the consistency between the imagery and the ground-truth datasets in a number of ways. Firstly, the grapevine vigour immediately after the fire and five months later can be significantly different. The canopy structure can either redevelop or decline further in several months' time post fire.

As a first assessment of the data before moving into modelling, the ground truth fire damage was compared with the immediate post-fire NDVI. This was done by calculating the correlation coefficient between the two.

As the fire damage data is ordinal (it falls into categories which can be ordered from best to worst), we made use of the Spearman's Rank Correlation Coefficient (ρ). As with other correlation coefficients, it lies between -1 and 1, where -1 denotes a perfect negatively monotonic relationship and 1 denotes a perfect positively monotonic relationship.

To minimise the inclusion of midrow and field edges, it was decided to work with the ground truth point data. However, as some misalignment may occur between the vine rows and the ground truth data, a buffer was created around each point of 1.5x1.8m. All pixels from the immediate post-fire image included in this buffer were then used in the correlation calculation. The associated ground truth fire damage classes were taken from the fire damage raster for each of the pixels. The resulting correlation coefficients can be seen in Table 6.2.3.

Table 6.2.3. Correlation coefficient between immediate post-fire NDVI and fire damage class.

Vineyard Block	ρ	p value
CT-1	-0.14	<0.0001
CT-2	-0.51	<0.0001
CT-3	-0.19	<0.0001
CT-4	-0.48	<0.0001
CT-5	0.04	<0.0001
CT-6	-0.08	<0.0001
CT-7	-0.25	<0.0001
CT-8	-0.09	<0.0001
CT-9	-0.59	<0.0001
CT-10 (March 2020 imagery)	-0.16	<0.0001
CT-11 (March 2020 imagery)	-0.14	<0.0001
CT-12	-0.46	<0.0001
CT-13	-0.18	<0.0001
CT-14	-0.39	<0.0001
CT-15	-0.48	<0.0001
CT-16	-0.46	<0.0001
CT-17	-0.70	<0.0001
CT-18	-0.53	<0.0001
CT-19	-0.49	<0.0001
CT-20	-0.29	<0.0001
CT-21	-0.43	<0.0001
CT-22	-0.47	<0.0001
CT-23	-0.66	<0.0001

The negative correlations found in Table 6.2.3 are expected as NDVI indicates plant health with a value closer to one indicating healthier vegetation and higher class label values indicate more damage, thus, we would expect them to have a lower NDVI generating an inverse relationship. The very low valued positive correlation for CT-5 reveals that no correlation was found as a zero value indicates no relationship between NDVI and fire damage.

The low correlation values for CT-10 and CT-11 are not unexpected as the post-fire image date is in March 2020 and it is expected that some regrowth would have already occurred by that time. As such, it is expected that the models developed later will not achieve very good results on these vineyard blocks.

Some of the lower correlations could be related to the delayed ground truth sampling of the vineyard blocks (see Table 6.2.3) and the estimation of damage immediately post fire. As mentioned previously, this would be a tricky task and the delay may render the ground truthing for some blocks inaccurate. In particular, for CT-5, 6 and 8, a visual examination of the immediate post fire image does not appear to match up with the ground truth data (See Figure 6.2.1).

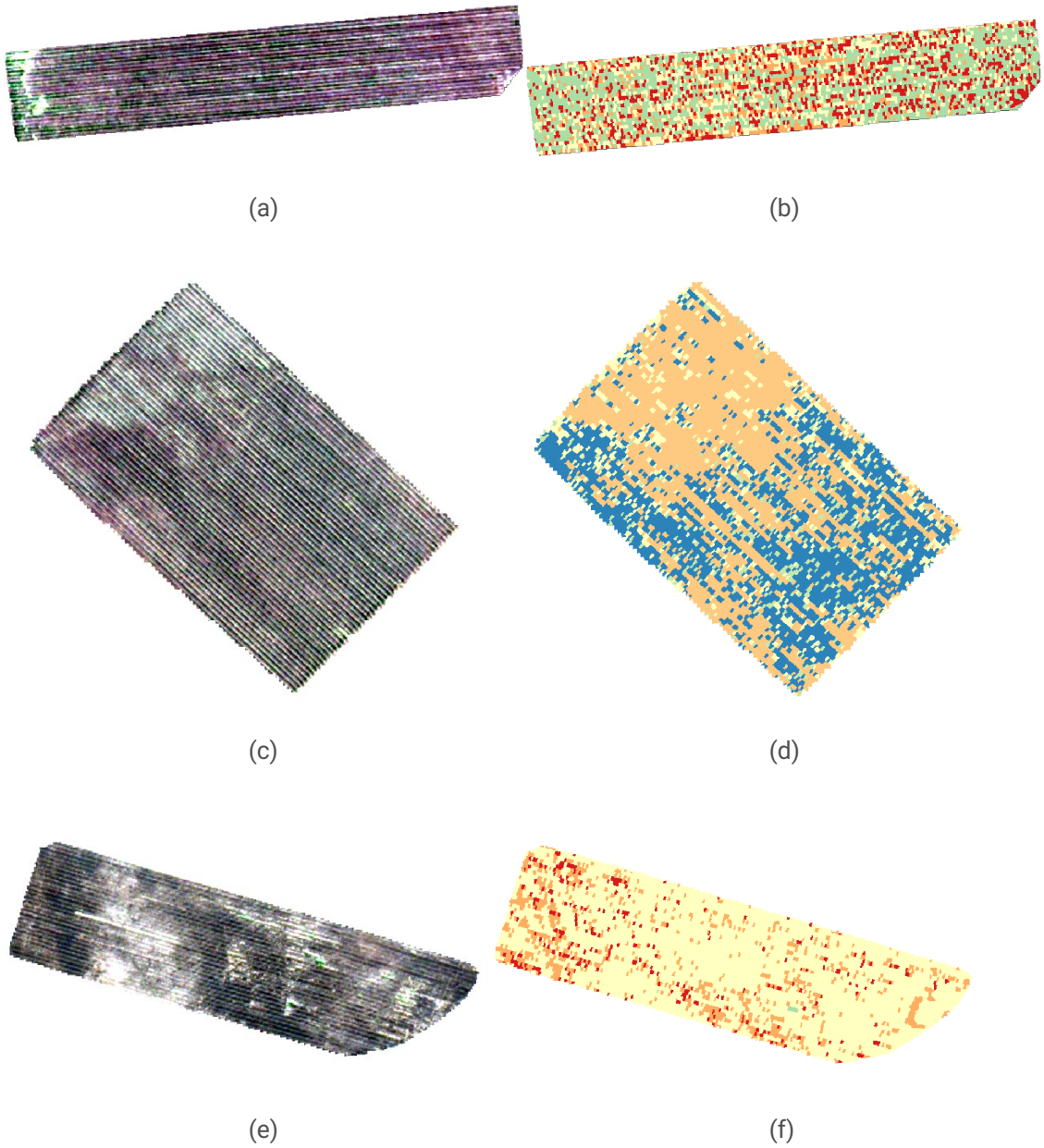


Figure 6.2.1. Immediate post fire satellite imagery (a,c,e) and ground truth sampling raster (b,d,f) for CT-5, CT-6 and CT-8 respectively. The ground truthing colours range from blue to red indicating no damage through to no growth.

Due to the narrow nature of vine rows in terms of pixels (each pixel is 0.5x0.5m), it is often not possible to exactly align the data such that all sample points are perfectly on a vine row. For supervised algorithms, this could present a problem in that the extracted training points could include a combination of mid row and vine row information. For unsupervised algorithms, this is less of a problem, however, unsupervised algorithms require a further step to assign a damage level (either binary or severity) to the groupings of pixels.

As severity data was collected some months post-fire, it may not be a true reflection of the original damage level. While every care was taken to best estimate what the severity of damage may have been just after the fire, with regrowth it would be a tricky task. While most immediate post-fire imagery is from the end of December 2019, for two of the vineyard blocks the first available image was from March 2020 (see Table 3). This creates a disconnect between the ground truth and the imagery and thus, it is not expected that a model trained on imagery immediately post-fire would perform well on an image captured four months later.

While not necessarily a concern or issue, it is important to note that for supervised learning, only four bands from the satellite imagery (red, green, blue and near infrared) can be used. While some of the available satellite images come from sensors which offer additional bands, as much of the imagery immediately post fire only contains these bands, the additional bands cannot be used.

6.2.2 Modelling of burn severity from satellite imagery

Unsupervised learning models

Given the previously mentioned concerns with the ground truth data set, it is challenging to build precise supervised learning models for the prediction. However, an unsupervised learning approach can be a good fit, since it does not require ground truth for the model building, and thus, inaccurate ground truth does not negatively affect the model. An unsupervised learning approach, HDBScan, typically clusters data points into different groups, based on the distance between data points.

Table 6.2.4. F1-score for the clustering approach

Vineyard Block	**F1-Score**	
	3 Class Model	Binary Model
CT-2	0.62	0.68
CT-3	0.70	0.77
CT-12	0.77	0.77
CT-14	0.27	0.28
CT-15	0.40	0.25
CT-16	0.20	0.31
CT-17	0.62	0.77
CT-21	0.56	0.48
CT-23	0.57	**0.88**
Average	0.52	0.58

Table 6.2.4 shows the performance of the unsupervised learning approach, HDBScan. It performs well on some blocks, e.g., CT-23 and CT-17, but not all (e.g., CT-15 and CT-16). In Figures 6.2.2 and 6.2.3, two blocks have been selected as examples to display the clustering results. It is another good way to evaluate the performance of the model. In general, the clustering model has captured most signals from satellite images, if comparing clustering results and raw images. It also clearly shows that ground truthing is not essential to determine the extent of fire damage via an unsupervised learning approach unless a quantitative assessment on fire damage is required.

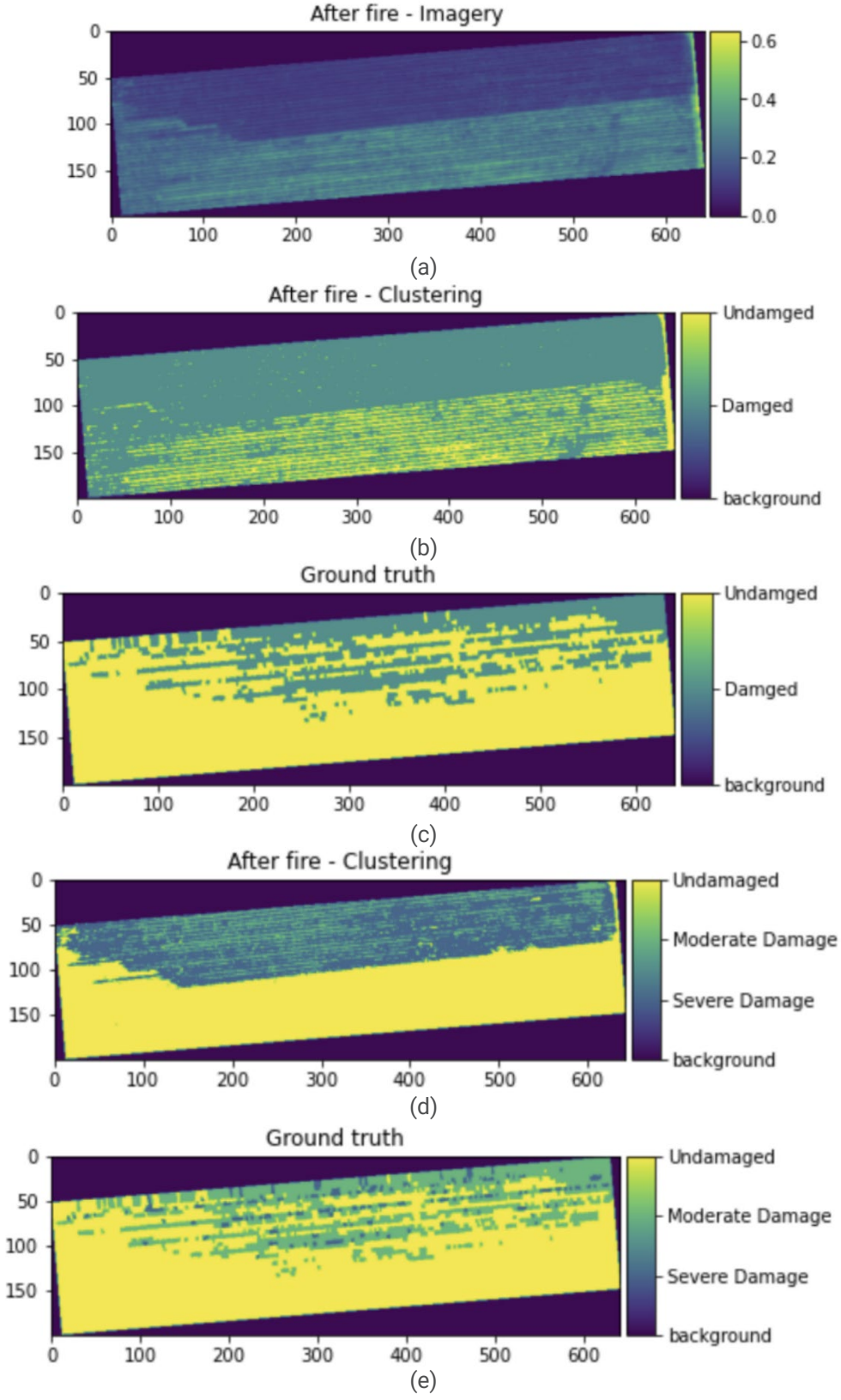


Figure 6.2.2. (a) Immediate post-fire image, (b) clustering results - 2 classes, (c) ground truth - 2 classes, (d) clustering results - 3 classes, and (e) ground truth - 3 classes for block CT-3.

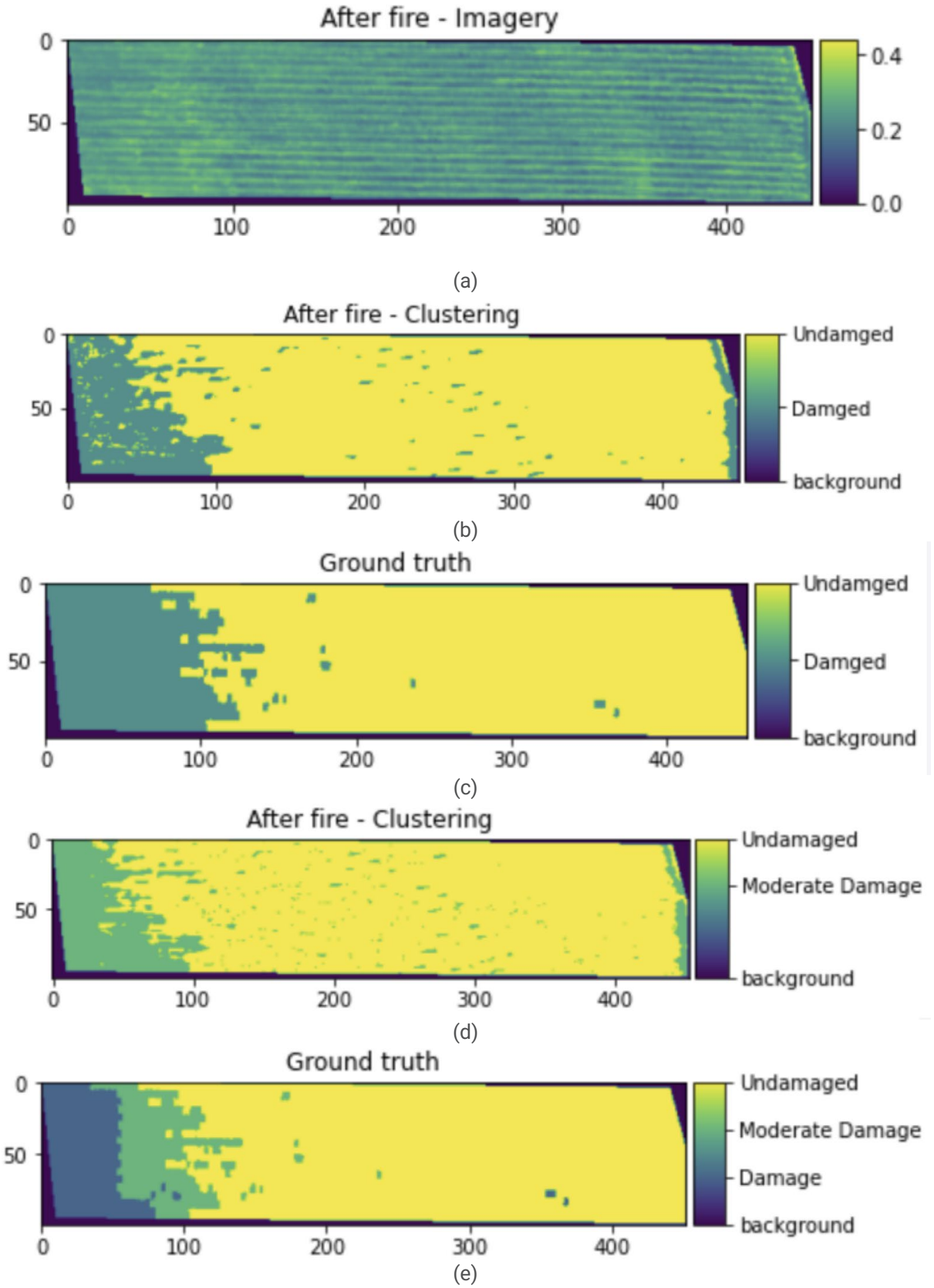


Figure 6.2.3. (a) Immediate post-fire image, (b) clustering results - 2 classes, (c) ground truth - 2 classes, (d) clustering results - 3 classes, and (e) ground truth - 3 classes for block CT-23.

In the undamaged section of CT-3 (Figure 6.2.2), the ground truth points match the raw satellite image well, but not for the damaged areas. However, the clustering model successfully reflected the damage determined from the satellite image. In CT-23 (Figure 6.2.3), the ground truth data matches the image quite well. The model successfully detected the damaged area.

Quadratic Discriminant Analysis

To facilitate testing on 3 class and binary models, datasets were produced with amended damage class labels. This relabelling occurred prior to training, testing and validation of the models but after the chosen vineyard blocks for training and testing were split. These 3 class and binary classifications as well as their relations to the original 5 classes can be seen in Table 6.2.5.

Table 6.2.5. Additional adopted Consilium Technology fire damage classification schemes.

Label	Classification	Old Classes
3 Class Classification		
0	Undamaged	Undamaged and Minor Damage
1	Moderate Damage	Moderate Damaged
2	Severe Damage	Severely Damaged and No Growth
Binary Classification		
0	Undamaged	Undamaged, Minor Damage
1	Damaged	Moderate Damage, Severely Damaged and No Growth

Quadratic Discriminant Analysis (QDA) is a classification algorithm which assumes that each class is normally distributed. Using this assumption and prior knowledge on the probability of each class, it calculates the probability that an observation belongs to each of the classes. The observation is then assigned to the class which it has the highest probability of belonging to.

The weighted average F1-score for all vineyard blocks can be seen in Table 6.2.6. It is important to note that the model was trained on CT-17 and CT-23 and thus, the higher values for these blocks is expected. The average accuracy of binary model is 0.79, and the model generated great results on some blocks, e.g. CT-14, CT-15 and CT-12.

Table 6.2.6. F1-score for Quadratic Discriminant Analysis for each vineyard block for 5, 3 and 2 class models. Note that F1-score here indicates a weighted average F1-score on all classes.

Vineyard Block	F1-Score		
	5 Class Model	**3 Class Model**	**Binary Model**
CT-2	0.34	0.60	0.74
CT-3	0.70	0.70	0.78
CT-12	0.54	0.67	**0.82**
CT-14	0.71	0.77	**0.83**
CT-15	0.34	0.56	**0.82**
CT-16	0.43	0.50	**0.80**
CT-17 (used to train)	0.64	0.73	**0.93**
CT-21	0.31	0.67	0.77
CT-23 (used to train)	0.57	**0.85**	**0.92**
Average (train)	0.61	0.79	**0.93**
Average (test)	0.48	0.64	0.79

Due to the number of blocks and use of three models, figures are only presented for CT-3 and 5 (Figures 6.2.4 and 6.2.5 respectively). Additionally, for ease of visualisation, the results are presented in a raster format. These images are generated from the point output by means of the nearest neighbours algorithm. This is the same process as was used for the original ground truth raster images.

For vineyard block CT-3, the zones generally match although the model is more extreme in the level of damage. This results in a good match once at a binary level. The ground truth for vineyard block CT-5 doesn't match the visual from the satellite image immediately post-fire well and this is likely due to regrowth before ground truth sampling took place and the estimation required to approximate what the damage would have been immediately post-fire. However, the model results do match up fairly well with the satellite imagery.

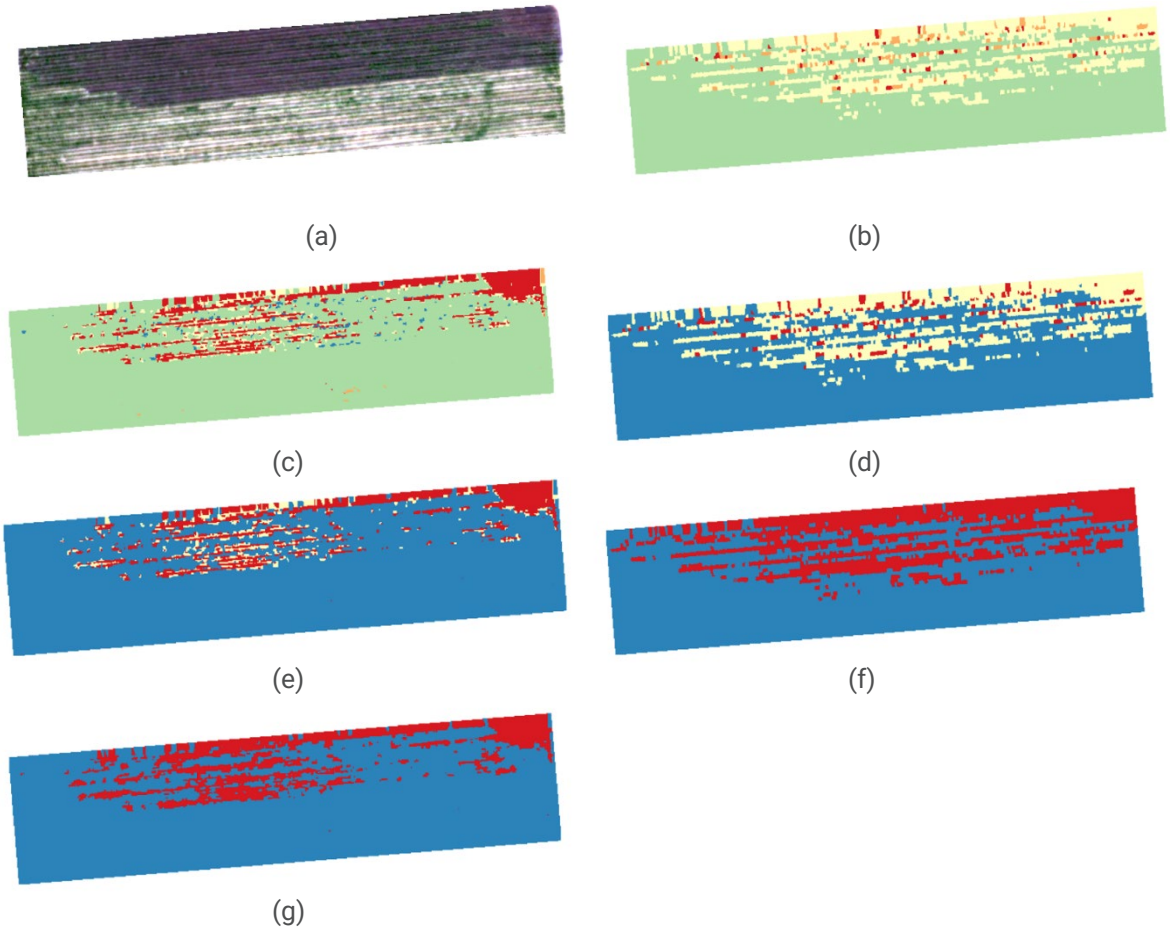


Figure 6.2.4. (a) Immediate post fire satellite imagery, (b) ground truth sampling raster - 5 classes, (c) 5 class model result, (d) ground truth sampling raster - 3 classes, (e) 3 class model result , (f) ground truth sampling raster - binary and (g) binary model result for CT-3. The ground truthing colours range from blue to red indicating no damage through to no growth.

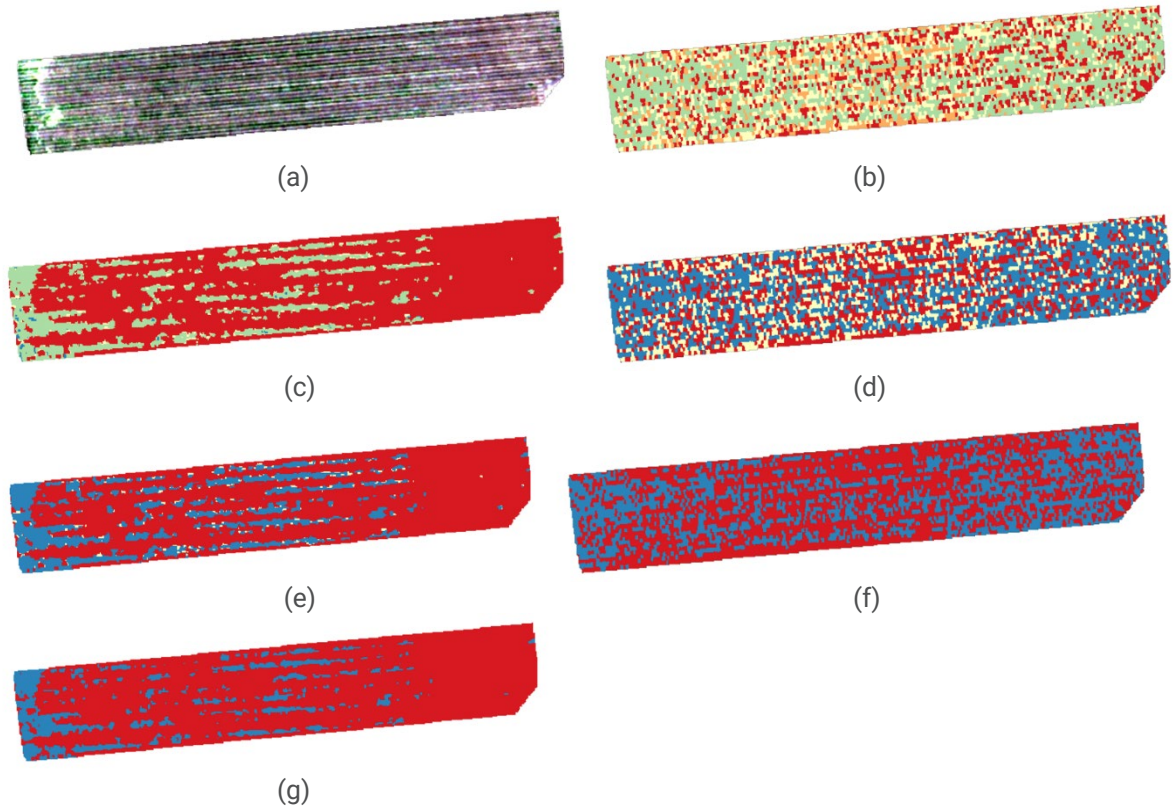


Figure 6.2.5. (a) Immediate post fire satellite imagery, (b) ground truth sampling raster - 5 classes, (c) 5 class model result, (d) ground truth sampling raster - 3 classes, (e) 3 class model result, (f) ground truth sampling raster - binary and (g) binary model result for CT-5. The ground truthing colours range from blue to red indicating no damage through to no growth.

XGBoost

XGBoost has been applied to making predictions on the CT data, including both binary classification (undamaged and damaged) and multi-classification (undamaged, minor damaged and major damaged).

Table 6.2.7 shows the average F1-score on both binary and 3 class models. One observation is that in both models the accuracy in training and testing data is roughly the same, which means that data used for training is representative of the testing data and the model does fit the data well. We can see that the binary model achieved a very good performance with more than 0.8 accuracy. The 3-class model got 0.65 accuracy on testing data, which is significantly higher than the random guess (the accuracy of the random guess in 3 class problems is 0.33).

Table 6.2.7. F1-score for XGBoost (cross validation) for each vineyard block for 3 and 2 class models. Note that F1-score here indicates a weighted average F1-score on all classes.

Models	Data	Average F1-Score
3 Class Model	Training	0.66
	Testing	0.65
Binary Model	Training	0.81
	Testing	0.81

As mentioned above, CT-17 and CT-23 have the ground truth well matched with the raw images, so they can be used as the training data to build the predictive models.

For binary classification, a good practice to evaluate the model performance is to visualize the prediction probability of each class, which can also be considered as the confidence of the predictions. For example, given a sample, the model may return the probability of 0.81 and 0.19 for classes 1 and 0. It means that the model has 81% confidence to classify the sample as class 1, and 19% as class 0. It obviously provides a better presentation of the prediction results.

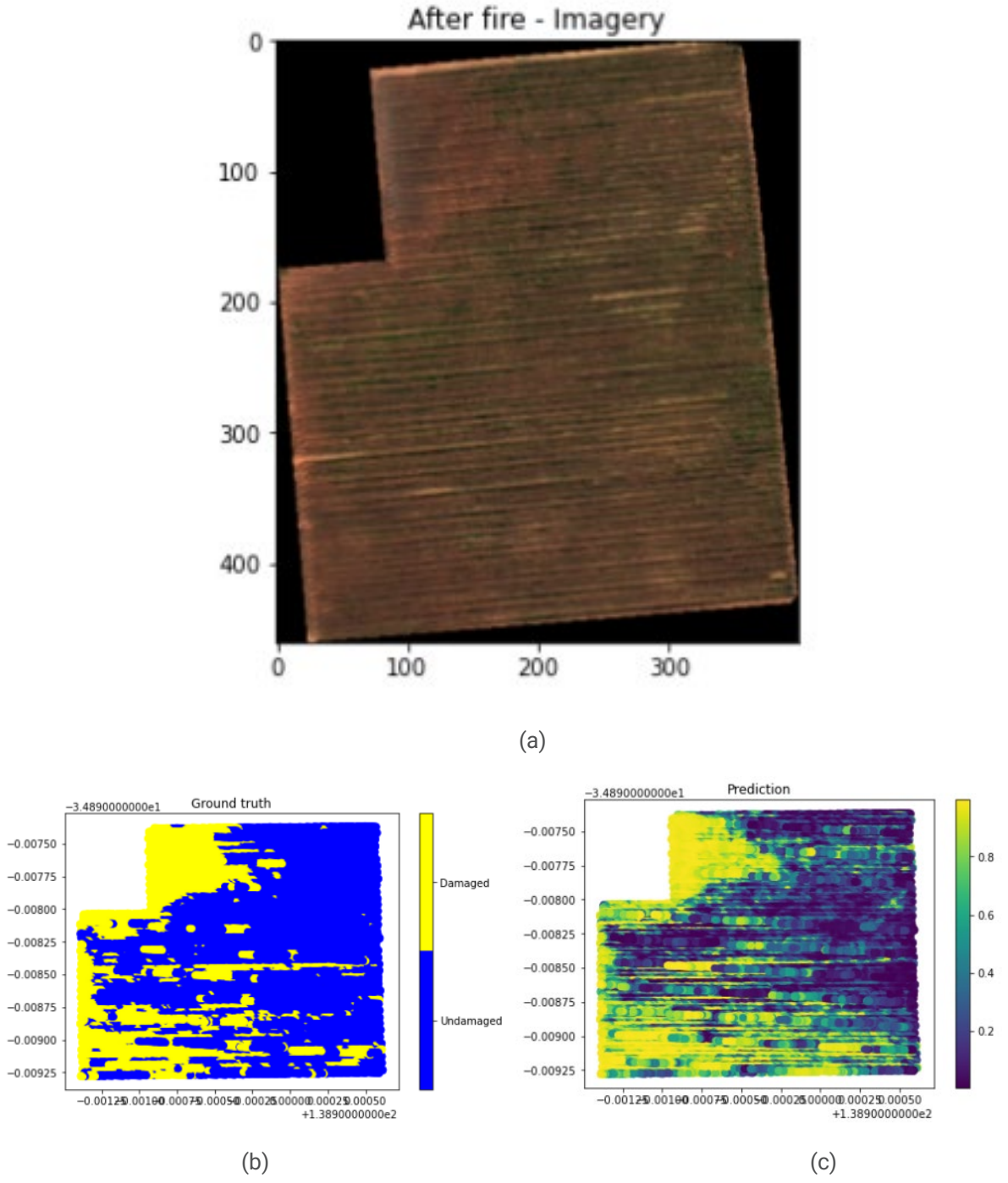
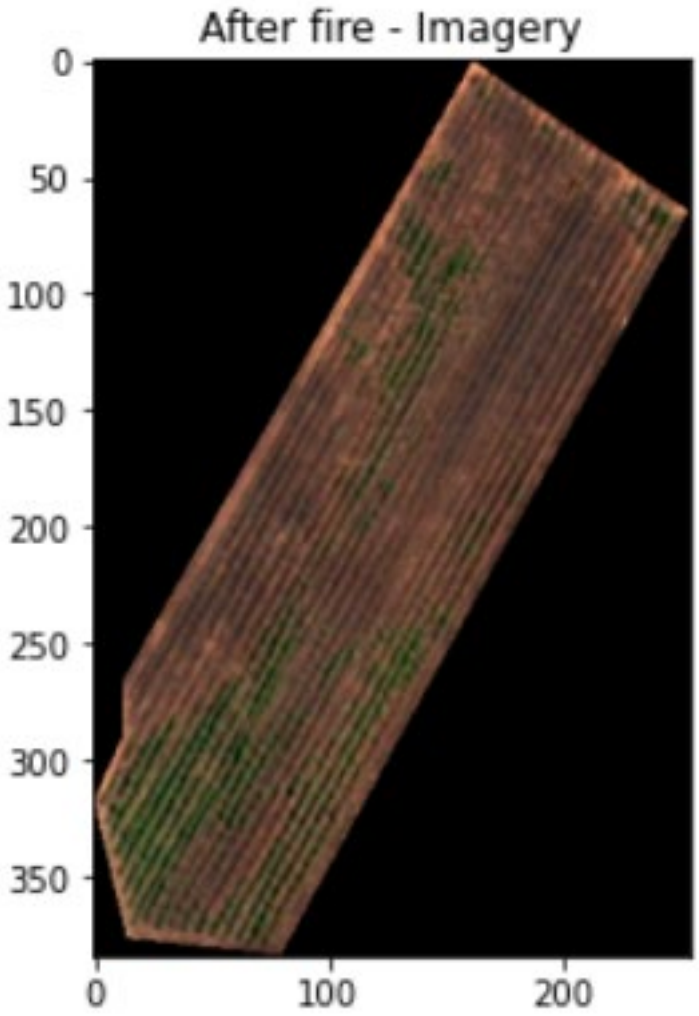
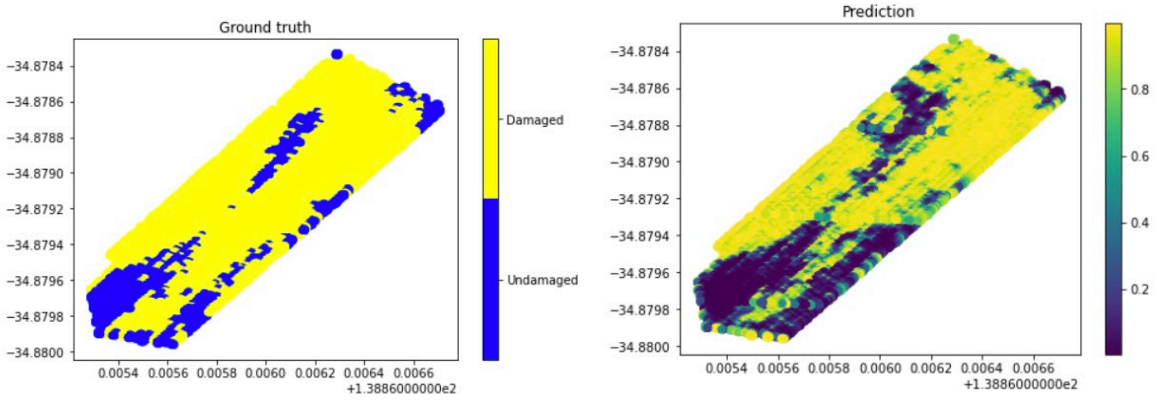


Figure 6.2.6. (a) Immediate post-fire image, (b) ground truth - 2 classes, (c) prediction - probability for block CT-2



(a)



(b) (c)

Figure 6.2.7. (a) Immediate post-fire image, (b) ground truth - 2 classes, (c) prediction - probability for block CT-15

The above two figures show the comparison of ground truth and predictions. In the prediction figures, a high value means a high confidence of a damaged vine, while a low value means a low confidence to classify it as damaged (that is, a high confidence to classify it as undamaged). We can see that the predictions match the raw image and the ground truth well.

6.2.3 Damage ratio

Immediately following a fire, it is useful for growers to know an estimate of the percentage of vines have been damaged by the bushfire. Table 6.2.8 shows the comparison of damage ratio between actual and predicted damage, and the corresponding absolute error. We can see that in most blocks, our model had less than 10% absolute error, where five (of nine) blocks reached a less than 5% error. In the testing data, the average absolute error (mean absolute error) is 7.65%. Given the limitation of ground truth quality and the small amount of data, this Mean Absolute Error is acceptable.

Table 6.2.8. Damage ratio for XGBoost for each vineyard block.

Vineyard Block	**Damage Ratio**		
	Actual	Predicted	Absolute Error
CT-2	30.58%	39.93%	**9.35%**
CT-3	24.96%	14.92%	10.04%
CT-12	25.72%	26.22%	**0.50%**
CT-14	18.19%	17.56%	**0.63%**
CT-15	78.95%	62.84%	16.11%
CT-16	73.97%	76.99%	**3.02%**
CT-17 (train)	68.22%	65.70%	**2.52%**
CT-21	28.87%	14.93%	13.94%
CT-23 (train)	22.96%	22.24%	**0.72%**
Average (train)	-	-	**1.62%**
Average (test)	-	-	**7.65%**

6.2.4 Summary

Both unsupervised learning and supervised learning approaches have been performed to predict the damage to grapevines from bushfire. An unsupervised learning approach, HDBScan, generated acceptable results. If no (high quality) ground truth data is available, then this approach provides acceptable results. Two supervised learning approaches, QDA and XGBoost, were also implemented to make predictions. Both provided good results and therefore have the potential to be applied to a larger area.

Table 6.2.9. Summary of scenarios calculated with CT data.

Scenario	Verdict
Unsupervised learning - HDBScan Clustering on every pixel of the satellite images	An unsupervised learning approach is useful when the quality of the ground truth data is poor, as in this study. The average F1 score is 0.58 and 0.52 on binary and 3 class data respectively. Although the F1 scores are not high, the visual comparison between raw images and clustering results does demonstrate the model's capacity to predict damage.
Supervised learning - Quadratic discriminant analysis Classifying pixels in a 1.5x1.8m buffer of each sampled vine	Pre-processing of data was performed to align pixels of each vine with the ground truth data to enable the supervised learning modelling. The average F1 score is 0.79 and 0.64 on binary and 3 class data, respectively. Results are reasonable, indicating that this method has the potential to be applied to a larger area.
Supervised learning - XGBoost Classifying pixels in a 1.5x1.8m buffer of each sampled vine 10-fold Cross validation on all samples	The average F1 score is 0.81 and 0.65 on binary and 3 class data respectively. Cross validation will randomly split data into training and testing sets, which can reduce many data quality issues. For example, some blocks have serious class imbalance problems, however cross validation can significantly reduce the class imbalance.
Supervised learning - XGBoost Classifying pixels in a 1.5x1.8m buffer of each sampled vine Training the model on two high quality blocks and testing on others	The average F1 score is 0.79 and 0.69 on binary and 3 class data, respectively. High quality data can help to build a better model and make better predictions. The average F1 scores look impressive, and it has the potential to be applied to a larger area.
Damage ratio Utilising trained XGBoost model to predict damage ratio	The mean absolute error of predicting damage ratio is 7.65%, where five (of nine) blocks reached a less than 5% absolute error. The results indicate that the method has the potential to be applied to a larger area.

6.3 Vine recovery after fire damage

6.3.1 Canopy Growth

To assess and monitor vine recovery, canopy growth was measured as PAI during the two seasons following the fire event (2020/21 and 2021/22) (Figures 6.3.1 and 6.3.2). In the first season (2020/21) after the fire, severely damaged vines at all sites, apart from site H had lower PAI at later stages of canopy development compared to those where no visible damage was observed. Vines classified as having minor-moderate fire damage had similar PAI at sites A, B, E, F, J to vines with no visible damage, while at site I, PAI values were similar to severely damaged vines and relatively low compared to other sites. PAI values at sites A and B in the second season (2021/22) were not different between any of the fire damage classifications. However, at site C only minor-moderately damaged vines had similar PAI levels to vines where no visible damage was observed. At sites D-F PAI for both minor-moderate and severely damaged vines was lower than no visible damage vines. Whereas at site H, no differences in PAI were observed between fire damage classifications at any time points in the two seasons following the bushfire.

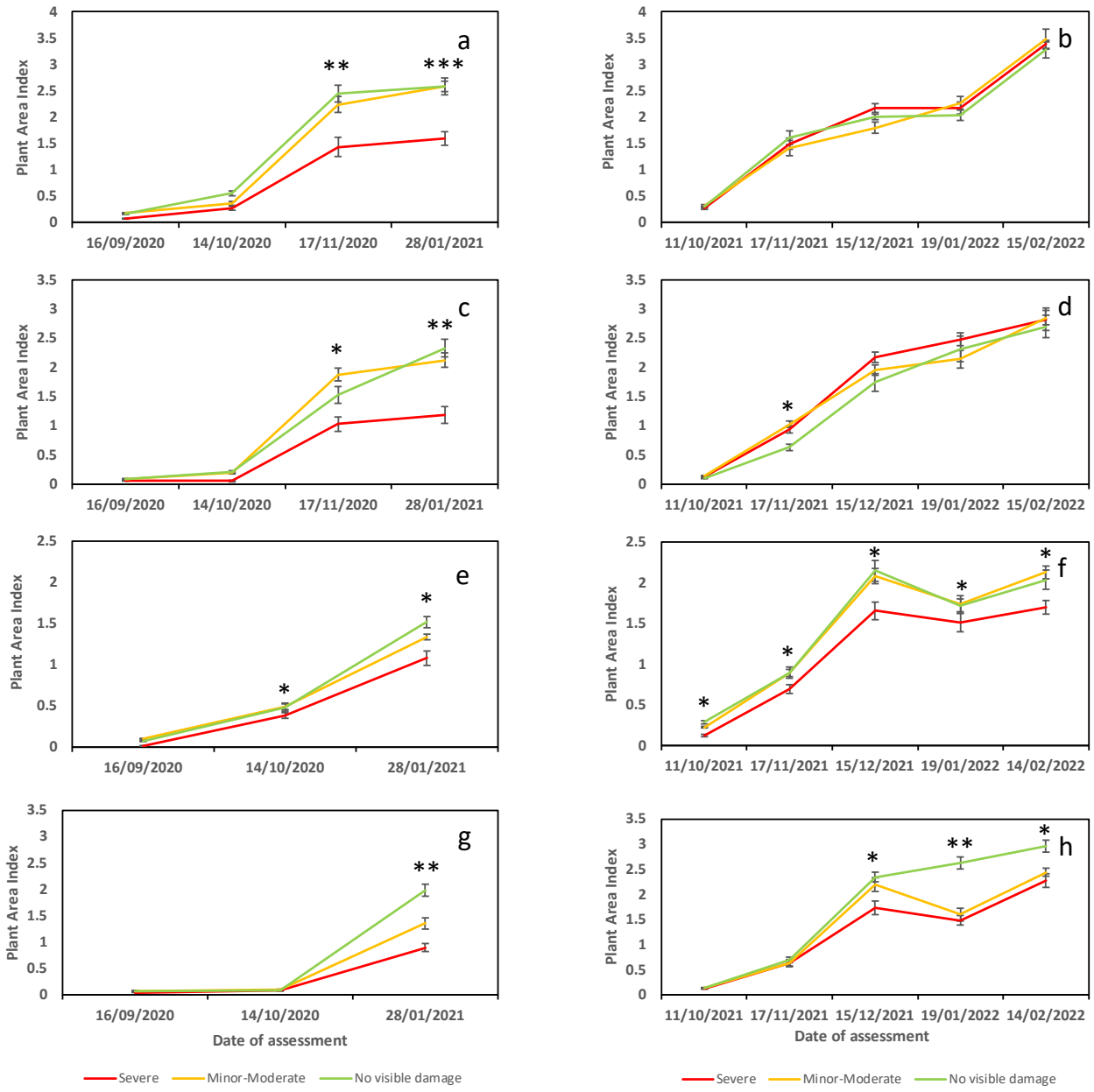


Figure 6.3.1. Plant Area Index measures of three different fire damage classifications; severe, minor-moderate and no visible damage at sites A (a and b), B (c and d), C (e and f) and D (g and h) from the 2020/21 and 2021/22 growing seasons, Adelaide Hills, South Australia. Fire damage classifications were analysed using one-way ANOVA. Each data point is a mean of n=12 vines. Bars indicate the standard error. *, ** and *** indicate significance at p ≤ 0.05, 0.01 and 0.0001 respectively, using the LSD test at 5% level.

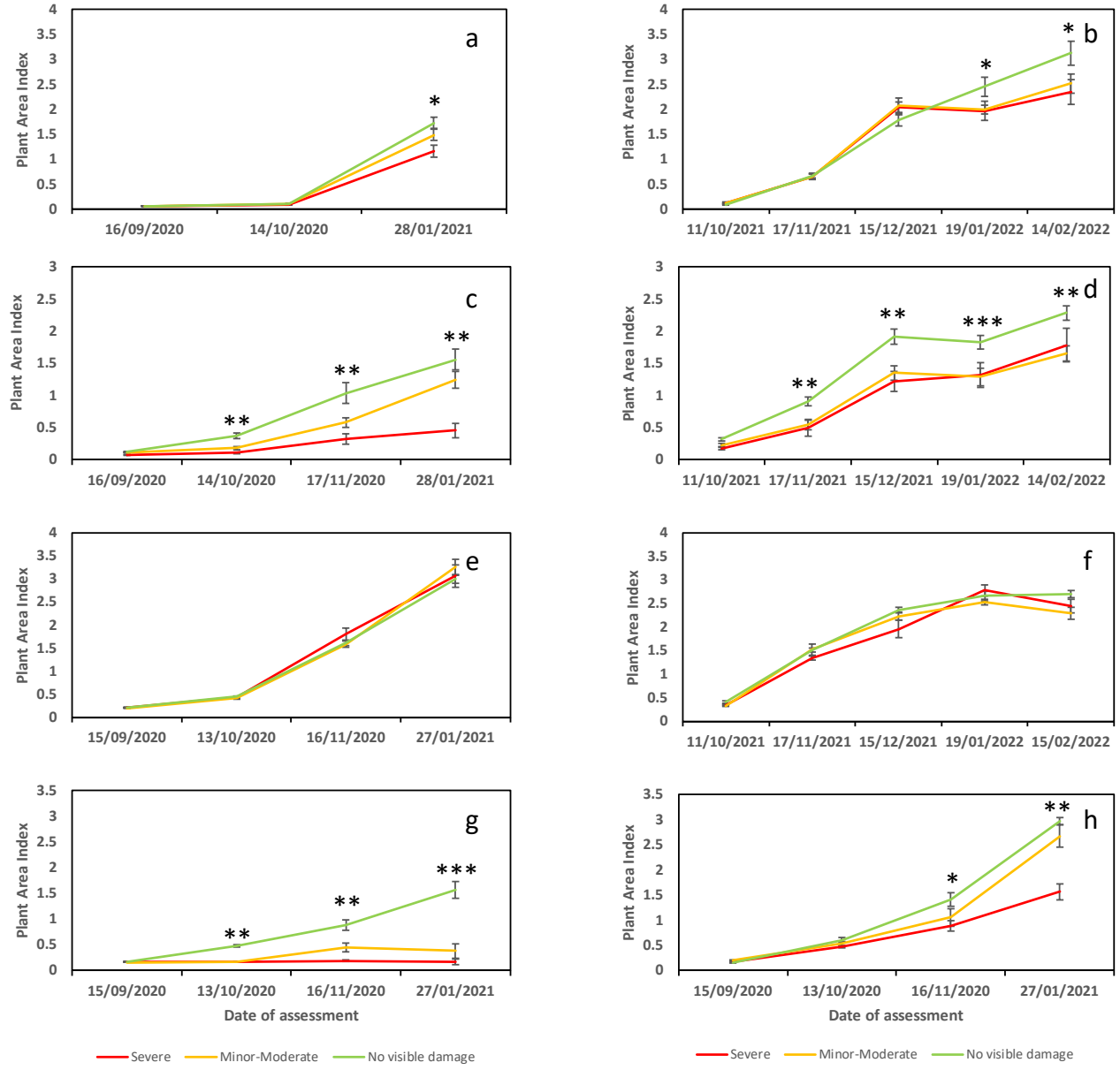


Figure 6.3.2. Plant Area Index measures of three different fire damage classifications severe, minor-moderate and no visible damage at sites E (a and b), F (c and d) and H (e and f) from the 2020/21 and 2021/22 growing seasons and sites I (g) and J (h) from the 2020/21 growing season (vineyards removed after first season), Adelaide Hills, South Australia. Fire damage classifications were analysed using one-way ANOVA. Each data point is a mean of n=12 vines. Bars indicate the standard error. *, ** and *** indicate significance at p ≤ 0.05, 0.01 and 0.0001 respectively, using the LSD test at 5% level.

6.3.2 Vine fertility and starch concentration

Seasonal differences in fertility were observed at some sites (Tables 6.3.1-6.3.3). Fruitfulness was higher in the second season at sites B-F (Tables 6.3.2.1 and 6.3.2). The cross-sectional area of inflorescence primordia (IA) was higher in the second season at sites A and D and lower at sites B and H, while bunch weight was lower in the second season at A, F and H and higher at sites D and E. Both berry number per bunch and berry weight were lower in the

second season at sites A and F. While berry weight was lower at site H. Higher berry numbers per bunch were observed at sites B-D and E in the second season and berry weight at sites C and F (Table 6.3.3).

Table 6.3.1. Inflorescence primordia number and area measures of buds from vines of different fire damage in two seasons following fire damage, 2020/21 and 2021/22, Adelaide Hills, South Australia.

		Variable					
		Inflorescence primordia number			**Inflorescence primordia area (μm)**		
Site	**Level of fire damage**	2020/2021	2021/2022	*p* value	2020/2021	2021/2022	*p* value
A	No visible damage	**1.593a**	**1.092bc**	*<0.0001(D)*	**0.066a**	**0.063a**	*0.014(D)*
	Minor-moderate	**1.354ab**	**1.216bc**	*ns (S)*	**0.065a**	**0.067a**	*<0.0001(S)*
	Severe	**0.526d**	**1.057c**	*<0.0001(DxS)*	**0.027b**	**0.074a**	*<0.0001(DxS)*
	Season	*1.157*	*1.22*		*0.053b*	*0.068a*	
B	No visible damage	**1.747a**	**1.260cd**	*<0.0001(D)*	**0.094a**	**0.055b**	*<0.0001(D)*
	Minor-moderate	**1.533ab**	**1.450bc**	*0.009(S)*	**0.105a**	**0.063b**	*0.012(S)*
	Severe	**0.157e**	**1.211d**	*<0.0001(DxS)*	**0.011c**	**0.062b**	*<0.0001(DxS)*
	Season	*1.146b*	*1.307a*		*0.070a*	*0.060b*	
C	No visible damage	**1.905a**	**1.769a**	*<0.0001(D)*	**0.131a**	**0.115a**	*<0.0001(D)*
	Minor-moderate	**1.580b**	**1.862a**	*0.012 (S)*	**0.125a**	**0.111a**	*ns (S)*
	Severe	**0.340c**	**1.321b**	*0.004 (DxS)*	**0.032c**	**0.076b**	*0.024 (DxS)*
	Season	*1.273b*	*1.650a*		*0.096*	*0.101*	
D	No visible damage	**0.908b**	**1.640a**	*ns (D)*	**0.074bc**	**0.085ab**	*ns (D)*
	Minor-moderate	**0.873b**	**1.681a**	*<0.0001(S)*	**0.068c**	**0.087ab**	*<0.0001(S)*
	Severe	**0.611c**	**1.508a**	*0.033(DxS)*	**0.050d**	**0.097a**	*0.003(DxS)*
	Season	*0.797b*	*1.610a*		*0.064b*	*0.089a*	
E	No visible damage	**0.905c**	**1.623ab**	*ns (D)*	**0.087a**	**0.070a**	*0.050(D)*
	Minor-moderate	**0.692cd**	**1.736a**	*<0.0001(S)*	**0.072a**	**0.075a**	*ns (S)*
	Severe	**0.532d**	**1.480b**	*0.010(DxS)*	**0.050b**	**0.073a**	*0.008(DxS)*
	Season	*0.709b*	*1.613a*		*0.070*	*0.073*	
F	No visible damage	**1.500a**	**0.867b**	*<0.0001(D)*	**0.115a**	**0.081b**	*<0.0001(D)*
	Minor-moderate	**0.817b**	**1.333a**	*<0.0001(S)*	**0.081b**	**0.082b**	*ns (S)*
	Severe	**0.000c**	**1.492a**	*<0.0001(DxS)*	**0.000c**	**0.083b**	*<0.0001(DxS)*
	Season	*0.772b*	*1.231a*		*0.065*	*0.068*	
G	No visible damage	**0.492a**	na	*<0.0001(D)*	**0.040a**	na	*<0.0001(D)*
	Minor-moderate	**0.108b**	na	*vineyard*	**0.008b**	na	*vineyard*
	Severe	**0.008b**	na	*removed*	**0.001b**	na	*removed before*
	Season			*before harvest*			*harvest*
H	No visible damage	1.47	1.50	*ns (D)*	0.078	0.073	*ns (D)*
	Minor-moderate	1.61	1.43	*ns (S)*	0.082	0.070	*0.008 (S)*
	Severe	1.56	1.34	*ns (DxS)*	0.090	0.074	*ns (DxS)*
	Season	*1.55*	*1.42*		*0.083a*	*0.072b*	
I	No visible damage	**1.397a**	na	*<0.0001(D)*	**0.090a**	na	*<0.0001(D)*
	Minor-moderate	**0.767b**	na	*one season*	**0.066b**	na	*one season*
	Severe	**0.025c**	na	*vineyard*	**0.002c**	na	*vineyard*
	Season			*removed*			*removed*
J	No visible damage	**1.420a**	na	*<0.0001(D)*	**0.108a**	na	*<0.0001(D)*
	Minor-moderate	**0.963b**	na	*one season*	**0.062b**	na	*one season*
	Severe	**0.650b**	na	*vineyard*	**0.043b**	na	*vineyard*
	Season			*removed*			*removed*

*na = not applicable, ns = not significant, *D* = fire damage assessment, *S* = season, *DxS* = fire level damage x season. Fire damage assessment and season effects and their interactions were analysed using a two-way ANOVA and the means separated with Tukey's test. Where vines were removed a one-way ANOVA was performed. Means followed by different letters are different at $p < 0.05$.

Table 6.3.2. Bunch number per shoot and bunch weight measures of vines of different fire damage in two seasons following fire damage, 2020/21 and 2021/22, Adelaide Hills, South Australia.

		Variable					
		Bunch number/shoot			Bunch weight (g)		
Site	**Level of fire damage**	2020/2021	2021/2022	*p* value	2020/2021	2021/2022	*p* value
A	No visible damage	**1.534a**	**1.113b**	*<0.0001(D)*	**147.6a**	**59.5c**	ns (D)
	Minor-moderate	**1.520a**	**1.159b**	*0.008(S)*	**135.8a**	**58.9c**	*<0.0001(S)*
	Severe	**0.546c**	**1.075b**	*<0.0001(DxS)*	**99.6b**	**66.8c**	*0.007(DxS)*
	Season	*1.200a*	*1.116b*		*127.6a*	*61.7b*	
B	No visible damage	**1.815a**	**1.231b**	*<0.0001(D)*	**94.9a**	**76.8b**	*<0.0001(D)*
	Minor-moderate	**1.654a**	**1.321b**	*ns (S)*	**69.9b**	**69.9b**	*0.019(S)*
	Severe	**0.285c**	**1.116b**	*<0.0001(DxS)*	**20.1d**	**53.4c**	*<0.0001(DxS)*
	Season	*1.251*	*1.235*		*54.9*	*66.7*	
C	No visible damage	**1.862a**	**1.810a**	*<0.0001(D)*	**65.1a**	**57.2a**	*0.0008(D)*
	Minor-moderate	**1.512b**	**1.853a**	*0.032(S)*	**55.3a**	**43.3b**	*ns (S)*
	Severe	**0.451c**	**1.212b**	*0.004 (DxS)*	**36.0b**	**42.1b**	*0.004 (DxS)*
	Season	*1.275b*	*1.625a*		*52.1*	*47.5*	
D	No visible damage	**0.888b**	**1.545a**	*<0.0001(D)*	43.5	77.6	*ns (D)*
	Minor-moderate	**0.835b**	**1.610a**	*<0.0001(S)*	44.8	86.1	*<0.0001(S)*
	Severe	**0.582c**	**1.510a**	*<0.0001(DxS)*	61.9	76.0	*ns (DxS)*
	Season	*0.768b*	*1.555a*		*50.0b*	*79.9a*	
E	No visible damage	**0.912c**	**1.677a**	*<0.0001(D)*	39.6	82.9	*ns (D)*
	Minor-moderate	**0.721c**	**1.712a**	*<0.0001(S)*	39.8	86.1	*<0.0001(S)*
	Severe	**0.433d**	**1.399b**	*<0.0001(DxS)*	47.4	83.8	*ns (DxS)*
	Season	*0.689b*	*1.598a*		*42.3b*	*84.2a*	
F	No visible damage	**1.521a**	**1.012b**	*<0.0001(D)*	**114.9a**	**68.6b**	*ns (D)*
	Minor-moderate	**0.912b**	**1.392a**	*0.0008(S)*	**73.8b**	**79.4b**	*0.037(S)*
	Severe	**0.000c**	**1.451a**	*<0.0001(DxS)*	**84.2b**	**78.5b**	*0.012(DxS)*
	Season	*0.811b*	*1.285a*		*91.0a*	*75.5b*	
G	No visible damage	na	na	*vineyard*	na	na	*vineyard*
	Minor-moderate	na	na	*removed before*	na	na	*removed before*
	Severe	na	na	*harvest*	na	na	*harvest*
	Season						
H	No visible damage	1.512	1.451	*ns (D)*	**107.5a**	**78.5b**	*0.008(D)*
	Minor-moderate	1.621	1.563	*ns (S)*	**115.0a**	**54.6b**	*0.0001(S)*
	Severe	1.593	1.421	*ns (DxS)*	**75.2b**	**57.5b**	*0.039(DxS)*
	Season	*1.574*	*1.484*		*99.2a*	*63.5b*	
I	No visible damage	**1.456a**	na	*<0.0001(D)*	**119.2a**	na	*<0.0001(D)*
	Minor-moderate	**0.751b**	na	*one season*	**84.2b**	na	*one season*
	Severe	**0.036c**	na	*vineyard*	**13.3c**	na	*vineyard*
	Season			*removed*			*removed*
J	No visible damage	**1.399a**	na	*<0.0001(D)*	**105.6a**	na	*<0.0001(D)*
	Minor-moderate	**0.914b**	na	*one season*	**67.2b**	na	*one season*
	Severe	**0.613c**	na	*vineyard*	**30.1c**	na	*vineyard*
	Season			*removed*			*removed*

*na = not applicable, ns = not significant, *D* = fire damage assessment, *S* = season, *DxS* = fire level damage x season. Fire damage assessment and season effects and their interactions were analysed using a two-way ANOVA and the means separated with Tukey's test. Where vines were removed a one-way ANOVA was performed. Means followed by different letters are different at $p < 0.05$.

Table 6.3.3. Berry number per bunch and berry weight measures from bunches of vines of different fire damage in two seasons following fire damage, 2020/21 and 2021/22, Adelaide Hills, South Australia.

		Variable					
		Berry number per bunch			Berry weight (g)		
Site	**Level of fire damage**	2020/2021	2021/2022	*p* value	2020/2021	2021/2022	*p* value
A	No visible damage	**125.1a**	**93.7bc**	*0.010(D)*	**1.143b**	**0.637c**	*0.014(D)*
	Minor-moderate	**111.6ab**	**85.7c**	*0.05(S)*	**1.193b**	**0.678c**	*<0.0001(S)*
	Severe	**74.9c**	**89.2bc**	*0.023(DxS)*	**1.268a**	**0.704c**	*ns (DxS)*
	Season	*103.8a*	*89.5b*		*1.201a*	*0.673b*	
B	No visible damage	**91.2a**	**106.3a**	*<0.0001(D)*	**0.997a**	**0.696b**	*<0.0001(D)*
	Minor-moderate	**61.7b**	**91.8a**	*<0.0001(S)*	**1.131a**	**0.733b**	*ns (S)*
	Severe	**20.6c**	**97.9a**	*<0.0001(DxS)*	**0.407c**	**0.506c**	*<0.0001(DxS)*
	Season	*50.9b*	*98.7a*		*0.709*	*0.645*	
C	No visible damage	**72.3a**	**115.5a**	*0.026(D)*	**0.734a**	**0.492c**	*0.007(D)*
	Minor-moderate	**81.7a**	**91.6b**	*0.045(S)*	**0.752a**	**0.485c**	*0.002(S)*
	Severe	**58.6b**	**86.6b**	*0.011(DxS)*	**0.566b**	**0.432c**	*0.004(DxS)*
	Season	*70.9b*	*97.9a*		*0.683a*	*0.469b*	
D	No visible damage	**77.7c**	**133.7a**	*ns (D)*	**0.665ab**	**0.580bc**	*0.016(D)*
	Minor-moderate	**76.0c**	**125.4ab**	*<0.0001(S)*	**0.558c**	**0.662ab**	*ns (S)*
	Severe	**61.3c**	**105.1b**	*0.050(DxS)*	**0.734a**	**0.672ab**	*0.013(DxS)*
	Season	*76.0b*	*125.3a*		*0.652*	*0.638*	
E	No visible damage	**80.1b**	**115.4a**	*0.034(D)*	**0.698a**	**0.681a**	*0.004(D)*
	Minor-moderate	**51.7c**	**96.3a**	*<0.0001(S)*	**0.711a**	**0.651a**	*ns (S)*
	Severe	**52.6c**	**115.7a**	*<0.0001(DxS)*	**0.512b**	**0.684a**	*<0.0001(DxS)*
	Season	*61.7b*	*109.1a*		*0.640*	*0.672*	
F	No visible damage	**121.8a**	**93.6bc**	*ns (D)*	**0.915b**	**0.725cd**	*ns (D)*
	Minor-moderate	**78.8c**	**110.3ab**	*ns (S)*	**0.878bc**	**0.711d**	*<0.0001(S)*
	Severe	**74.0c**	**111.5ab**	*0.001(DxS)*	**1.087a**	**0.675d**	*0.05(DxS)*
	Season	*91.5*	*105.1*		*0.960a*	*0.704b*	
G	No visible damage	na	na	*vineyard*	na	na	*vineyard*
	Minor-moderate	na	na	*removed*	na	na	*removed before*
	Severe	na	na	*before harvest*	na	na	*harvest*
	Season						
H	No visible damage	88.7	95.7	*ns (D)*	1.148ab	0.781c	*ns (D)*
	Minor-moderate	93.7	67.8	*ns (S)*	1.311a	0.759c	*<0.0001(S)*
	Severe	86.1	77.2	*ns (DxS)*	0.920bc	0.742c	*ns (DxS)*
	Season	*89.5*	*80.2*		***1.126a***	***0.766b***	
I	No visible damage	**122.8a**	na	*<0.0001(D)*	**0.984a**	na	*0.0002(D)*
	Minor-moderate	**90.3b**	na	*one season*	**1.116a**	na	*one season*
	Severe	**21.3b**	na	*vineyard*	**0.451b**	na	*vineyard*
	Season			*removed*			*removed*
J	No visible damage	**113.6a**	na	*<0.0001(D)*	**0.906a**	na	*<0.0001(D)*
	Minor-moderate	**76.3b**	na	*one season*	**0.707b**	na	*one season*
	Severe	**18.8c**	na	*vineyard*	**0.541c**	na	*vineyard*
	Season			*removed*			*removed*

*na = not applicable, ns = not significant, *D* = fire damage assessment, *S* = season, *DxS* = fire level damage x season. Fire damage assessment and season effects and their interactions were analysed using a two-way ANOVA and the means separated with Tukey's test. Where vines were removed a one-way ANOVA was performed. Means followed by different letters are different at $p < 0.05$.

Vine fertility followed a similar trend to canopy growth (PAI) where fertility was reduced after fire damage, but at most sites recovery was seen in the second season (Tables 6.3.1- 6.3.3). Clear differences in inflorescence number between fire damage classes were observed at sites C, F and I with higher numbers of inflorescence primordia (IP) and greater IA for buds collected from no visible damage vines, followed by minor-moderate and then severe damage. At sites A, B, D and E, IP and IA were lower only for severely damaged vines and at sites G and J both minor-moderate and severely damaged vines had similar IP and IA values (Table 6.3.1). No differences in IP, IA, and bunch number per shoot were observed between levels of fire damage at site H; only bunch weight was lower for severely damaged vines in the first season. Bunch number per shoot and bunch weight aligned with IP and IA values at most sites (Table 6.3.2). Bunch number at sites A-D and bunch weight at A and F were not different between fire damage classes. Lower bunch weight, berry weight and berry number per bunch were observed in severely damaged vines at sites B and C in both seasons (Tables 6.3.2 and 6.3.3). In the first season, berry number per bunch was lowest in severely damaged vines at sites, A-C and J and berry weight at sites B-E, I and J. By the second season only lower berry weight was observed for severely damaged vines at site B and berry number per bunch at site C.

Bud and cane starch levels were higher in the second season for all sites apart from sites where vines were removed (Table 6.3.4). Cane starch was not different at sites A and H between fire damage classes (Table 6.3.4). Lower cane starch levels were observed in severely damaged vines at sites B-G, I and J in the first season and at sites C-F in the second season. While bud starch levels were lower in the first season at most sites (A-C, F, G, I and J) and at sites A-D in the second season. Minor-moderately damaged vines had lower bud starch levels at site D in the first season. Bud starch levels did not vary between fire damage classes at site H (Table 6.3.4).

6.3.3 Summary

After fire damage, vines have the ability to recover with time, however there are consequences in terms of canopy growth and development, vine fertility and starch reserves. The ability to recover and the speed of recovery appear to be related to the extent of initial fire damage. Cold-injury following freezing events elicits a similar response in grapevines (Wolfe 2001, Keller and Mills 2007). Canopy growth of vines in the first season following fire damage was consistently lower for vines that were classified as severely damaged at all sites, apart from at site H; which had the least fire damage of all sites. Interestingly, this pattern of growth development aligns with cane starch concentrations which were generally lower for vines that were severely damaged by the fire, particularly in the first season. Again, at site H no differences in cane or bud starch concentrations between fire damage classes were observed. As starch is known to be the main reserve compound in grapevine storage tissue (Winkler & Williams 1945) it makes sense that stress inflicted by the fire potentially reduced photosynthetic performance and reserve accumulation, with implications for canopy growth and development and yield in the following seasons (Hunter *et al.,* 1995). Only at sites A and B did the canopy growth fully recover by the second season, and at both of these sites additional water and nutrients were applied to the vines during the recovery phase, compared to other sites that maintained normal management practices. At sites D-F, both the vines classified as minor-moderate and severely damaged had lower PAI compared to those with no visible damage. While at site C it was only severely damaged vines that had a lower PAI. These patterns also align with overall fire damage at each of the sites, as can be seen in satellite imagery presented in Figures 6.1.3-6.1.5. It may be possible to improve recovery times by adapting viticultural management practices, such as pruning strategies, nutrient regimes and water management (Rose 2009; Whiting 2012; Collins *et al.,* 2013; Wang *et al.,* 2019; Hamilton, 2020). Experimental trials comparing different pruning strategies have been established and will be reported in future work.

Table 6.3.4. Bud and cane starch concentrations from vines of different fire damage in two seasons following fire damage, 2020/21 and 2021/22, Adelaide Hills, South Australia.

		Variable					
		Bud Starch (mg/g)			Cane Starch (mg/g)		
Site	**Level of fire damage**	2020/2021	2021/2022	*p* value	2020/2021	2021/2022	*p* value
A	No visible damage	**91.7bc**	**168.3a**	*ns (D)*	96.9	205.2	*ns (D)*
	Minor-moderate	**65.7cd**	**129.6ab**	*<0.0001 (S)*	90.8	160.4	*<0.0001(S)*
	Severe	**42.9d**	**113.1b**	*0.002(DxS)*	85.6	156.6	*ns (DxS)*
	Season	*66.7b*	*137.1a*		*91.1b*	*174.1a*	
B	No visible damage	**43.2c**	**86.8ab**	*0.005(D)*	**130.4bc**	**173.8a**	*<0.0001(D)*
	Minor-moderate	**49.9c**	**108.2a**	*<0.0001(S)*	**103.3c**	**176.5a**	*<0.0001(S)*
	Severe	**16.8d**	**79.9b**	*0.003(DxS)*	**33.2d**	**154.9a**	*0.002(DxS)*
	Season	*36.6b*	*91.6a*		*88.9b*	*168.4a*	
C	No visible damage	**76.0c**	**162.5a**	*<0.0001(D)*	**121.1b**	**191.6a**	*<0.0001(D)*
	Minor-moderate	**55.2d**	**158.6a**	*0.003(S)*	**120.9b**	**188.4a**	*0.002(S)*
	Severe	**27.9e**	**121.1b**	*0.002(DxS)*	**69.3c**	**136.9b**	*0.003(DxS)*
	Season	*53.1b*	*147.4a*		*103.7b*	*172.3a*	
D	No visible damage	**41.3c**	**120.2a**	*0.05 (D)*	**96.0c**	**219.7a**	*ns (D)*
	Minor-moderate	**34.6c**	**92.3b**	*<0.0001(S)*	**93.4c**	**206.6a**	*<0.0001(S)*
	Severe	**33.6c**	**88.3b**	*ns (DxS)*	**68.1d**	**198.0b**	*0.042 (DxS)*
	Season	*36.5b*	*100.3a*		*85.8b*	*208.1a*	
E	No visible damage	**56.5c**	**109.9a**	*ns (D)*	**121.9c**	**224.1a**	*ns (D)*
	Minor-moderate	**50.9c**	**113.2a**	*<0.0001(S)*	**114.4c**	**208.5a**	*<0.0001(S)*
	Severe	**50.7c**	**77.5a**	*0.008(DxS)*	**108.8c**	**176.1b**	*0.013(DxS)*
	Season	*52.7b*	*100.2a*		*115.0b*	*202.9a*	
F	No visible damage	**90.5a**	**93.5a**	*0.003(D)*	**108.4b**	**150.4a**	*<0.0001(D)*
	Minor-moderate	**75.3a**	**85.8a**	*0.003(S)*	**91.9b**	**134.0a**	*ns (S)*
	Severe	**32.9b**	**82.8a**	*0.003(DxS)*	**91.5b**	**110.5b**	*<0.0001(DxS)*
	Season	*66.2b*	*87.4a*		*97.3b*	*131.6a*	
G	No visible damage	**82.7a**	na	*0.002(D)*	**118.5a**	na	*ns (D)*
	Minor-moderate	**63.6a**	na	*vineyard*	**104.4a**	na	*vineyard*
	Severe	**39.7b**	na	*removed*	**94.3b**	na	*removed*
	Season			*before harvest*			*before harvest*
H	No visible damage	74.7	144.7	*ns (D)*	131.3	186.4	*ns (D)*
	Minor-moderate	69.4	143.8	*<0.0001(S)*	128.2	164.9	*<0.0001(S)*
	Severe	58.8	141.0	*ns (DxS)*	108.4	146.3	*ns (DxS)*
	Season	*67.6b*	*143.2a*		*125.9b*	*165.9a*	
I	No visible damage	**111.9a**	na	*0.013(D)*	**162.1a**	na	*0.044(D)*
	Minor-moderate	**96.4a**	na	*one season*	**148.7a**	na	*one season*
	Severe	**41.6b**	na	*vineyard*	**88.4b**	na	*vineyard*
	Season			*removed*			*removed*
J	No visible damage	**28.1a**	na	*0.05(D)*	**99.1a**	na	*0.038(D)*
	Minor-moderate	**20.8a**	na	*one season*	**90.2a**	na	*one season*
	Severe	**12.1b**	na	*vineyard*	**73.8b**	na	*vineyard*
	Season			*removed*			*removed*

*na = not applicable, ns = not significant, *D* = fire damage assessment, *S* = season, *DxS* = fire level damage x season. Fire damage assessment and season effects and their interactions were analysed using a two-way ANOVA and the means separated with Tukey's test. Where vines were removed a one-way ANOVA was performed. Means followed by different letters are different at $p < 0.05$.

A decrease in fruitfulness in the first season following the fire was observed at all sites (apart from site H) and particularly for vines that were severely damaged. Grapevine reproductive development occurs over two growing seasons (Iland *et al.,* 2011). It starts at floral induction, followed by initiation and differentiation of inflorescence primordia within buds in the first year, and further development of inflorescence in the second year until reaching bunch maturity

(May 2004). Hence the results found in this study are not surprising as when the fire occurred in December 2019 it coincided with the development of inflorescence primordia in the compound buds on the current season shoots. The conditions during the initiation and differentiation of IP in the current season are known to influence bud fruitfulness and potential yield (Li-Mallet *et al.,* 2016). In addition, a vine's reserves during development can influence bud fruitfulness as the actively growing shoot tips, young leaves and inflorescences strongly compete for reserves with the compound bud (Buttrose, 1966; Candolfi-Vasconcelos & Koblet, 1990). Hence, IP initiation and differentiation can be suppressed by limited reserves. This is supported by lower bud and cane starch levels reported in this study, particularly for severely damaged vines in the first season. Lower berry number per bunch and berry weights were observed and may also be attributed to the reserve status of the vines (Hunter *et al.,* 1995). At all sites, starch levels were higher in the second season (where measured) suggesting that strategies to improve storage accumulation in vines may be an important management approach to consider in order to shorten the recovery time.

7. Outcome/Conclusion

Quantifying the level of fire damage in vineyards after a fire event is currently time consuming and therefore makes accurate assessment difficult over a large area. The use of satellite imagery to overcome these issues was investigated through the comparison of vegetation indices (NDVI and VARIgreen) with ground truth measures of damage. However, only weak correlations were found with these two indices. This is likely due to the time difference between imagery and ground truth collection but it is possible that mixed pixels (containing both midrow and vine information) also contributed to the low correlations. However, as these are individual correlations between a single variable (NDVI or VARIgreen) and fire damage, further exploration using machine learning approaches may yield improved results. In the future, analysis of satellite imagery could also be supported by UAV imagery (Brook *et al.,* 2020).

Tracking vine recovery after a fire is critical to our understanding of the influence of different levels of fire damage on plant health. However, this is challenging as the varying degrees of fire damage are difficult to quantify, therefore this type of research is more observational rather than experimental in nature. This study allows inference to association rather than causation, and authors acknowledge that there may be other contributing factors that were not apparent. Regardless, the large differences in canopy growth and reproductive development between the different levels of fire damage are believed to be of value and interest to producers and managers as they provide some insights into the recovery process that can be used for vineyard management decision making.

Unfortunately, the extended time taken to collect the ground truth data meant that it was not suitable to generate multi class labels relating to degree of fire damage, however it was sufficient to create an indication of the fire scar and likely damage to vineyards. In future fire events, the models created through this project can be delivered as a service by Consilium Technology to governments or industry bodies to expedite strategic decisions and support delivered to affected growers.

COVID-19 proved a challenge with the broader extension of the project outputs, as the confidence to, or ability to, host in-person field days and conferences were limited.

8. Recommendations

Unfortunately, the interactions between fire severity/damage and vine recovery are still poorly known, especially at the scale of a large fire. Remote sensing imagery has been used to study the influence of fire severity on vegetation recovery (Díaz-Delgado & Pons 2001; Díaz-Delgado et al., 2003). Correlation between post fire NDVI and VARIgreen with fire damage was assessed as a first initial exploratory data analysis task due to the potential for delay in the fire damage assessment. Additional analysis such as considering the NDVI difference pre- and post-fire would likely be a better indicator of later model performance. Additionally, it is acknowledged, that considering a time series approach of the NDVI or other indices over several years for the same area at a similar time may well help define the 'normal' state of the particular vineyard block under consideration. The current approach also does not account for natural variability within the vineyard block. Due to variability in pre-fire NDVI, the assessment has been performed at the block level although if the difference in NDVI had been used, merging of the data from all blocks could have been considered. Satellite imagery tracking vineyard recovery in the seasons following the bushfire is also currently being correlated to field assessments of vineyard productivity such as canopy health and development, fertility and starch concentration. Studies by Cogato et al.,2021; Pinel et al.,2021; Lopez-Fornieles et al.,2022, are examples of strategies we can use to further explore these relationships.

The relatively small number of ground truth data sets limited the development of a highly accurate machine learning model. Furthermore, the delays of up to four months in gathering ground truth data, meant regrowth of vines impacted upon the reliability of the degree of damage data. This limited the ability to create a reliable multi- class variable damage model, however several models have been created capable of determining a binary estimation of fire damage in vineyards with relative confidence. In the event of future fires these models can be deployed soon after the event, and a co-ordinated collection of concurrent ground truth data can help form better data sets to improve accuracy and build variable damage models. Tools that rapidly and affordably capture the extent and severity of damage over large vineyard areas will allow producers and government and industry bodies to make more efficient recovery decisions post fire event. The benefits of this will include better fire recovery planning, coordination and delivery, providing more certainty and reducing stress.

9. Appendix 1: Communication

Communication and extension of the outcomes of research generated during this project are listed below:

Presentations

- Clarke, A., Collins, C., Ouyang, J., James, A., De Simoni, L., De Bei, R., Hinze, C., Wong, S. (2020). *Rapid assessment and grapevine recovery after a bushfire.* International Organisation of Vine and Wine Protection and Technology Experts Group (OIV PROTEC), June 26, 2020. *Oral presentation*
- Ouyang J., Collins, C., James, A., De Simoni, L., De Bei, R., Hinze, C., Wong, S., Clarke, A. (2020). *Rapid assessment and grapevine recovery after a bushfire.* Adelaide Hills Wine Region Technology Workshops, September 18, 2020. *Oral presentation*
- Clarke, A., Collins, C., Ouyang, J., James, A., De Simoni, L., De Bei, R., Hinze, C., Wong, S. (2020). *Rapid assessment and grapevine recovery after a bushfire.* Lien de la Vigne (Vinelink). December 1, 2020. *Oral presentation*
- Collins, C., Ouyang, J., James, A., De Simoni, L., De Bei, R., Hinze, C., Wong, S. Clarke, A. (2021). *Rapid assessment and grapevine recovery after a bushfire.* National wine sector bushfire conference, May 25, 2020. *Oral presentation*
- Collins, C., Ritchie, M., James, A., O'Brien, P., Ma, S., De Bei, R., and Clarke, A. (2022). Rapid damage assessment and grapevine recovery after fire. 18th Australian Wine Industry Technical Conference, Adelaide, 26-29 June 2022. *Poster Presentation*
- Collins, C., Ritchie, M., James, A., O'Brien, P., Ma, S., De Bei, R., and Clarke, A. (2022). Rapid damage assessment and grapevine recovery after fire. 18th Australian Wine Industry Technical Conference, Adelaide, 26-29 June 2022. *Oral Presentation*
- Collins, C., Ritchie, M., James, A., O'Brien, P., Ma, S., De Bei, R., and Clarke, A. (2022). Grapevine recovery after fire and a first look at rapid damage assessment with satellite imagery. TerClim22 (XIVth International Terroir Congress and 2nd ClimWine Symposium), 3-8 July 2022, Bordeaux, France. *Oral Presentation*

Journal articles

- Collins, C., Ritchie, M., James, A., O'Brien, P., Ma, S., De Bei, R., and Clarke, A. (2022). Grapevine recovery after fire and a first look at rapid damage assessment with satellite imagery. OENO One, 56 http://10.20870/oeno-one.2021.55.3.4730

10. Appendix 2: Intellectual Property

Project IP register supplied to Wine Australia

11. Appendix 3: References

Black, E., Greatrex, H., Young, M. & Maidment, R. (2016). Incorporating satellite data into weather index insurance. *Bulletin of the American Meteorological Society*, 97, ES203–ES206. https://doi.org/10.1175/BAMS-D-16-0148.1

Bokusheva, R., Kogan, F., Vitkovskaya, I., Conradt, S. & Batyrbayeva, M. (2016). Satellite-based vegetation health indices as a criteria for insuring against drought-related yield losses. *Agricultural and Forest Meteorology*, 220, 200–206. https://doi.org/10.1016/j.agrformet.2015.12.066

Brook, A., De Micco, V., Battipaglia, G., Erbaggio, A., Ludeno, G., Catapano, I. & Bonfante, A. (2020). A smart multiple spatial and temporal resolution system to support precision agriculture from satellite images: Proof of concept on Aglianico vineyard. *Remote Sensing of Environment*, 240, 111679. https://doi.org/10.1016/j.rse.2020.111679

Buttrose, M. (1966). Use of carbohydrate reserves during growth from cuttings of grape vine. *Australian Journal of Biological Sciences,* 19, 247-256. https://doi.org/10.1071/BI9660247

Candolfi-Vasconcelos, M.C. & Koblet, W. (1990). Yield, fruit quality, bud fertility and starch reserves of the wood as a function of leaf removal in *Vitis vinifera* -Evidence of compensation and stress recovering. *Vitis*, 29, 199-221.

Cogato, A., Meggio, F., Collins, C. & Marinello, F. (2020). Medium-resolution multispectral data from Sentinel-2 to assess the damage and the recovery time of late frost on vineyards. *Remote Sensing*, 12, 1896-1912. https://doi:10.3390/rs12111896

Cogato, A., Wu, L., Jewan, S.Y.Y., Meggio, F., Marinello, F., Sozzi, M. & Pagay, V. (2021). Evaluating the spectral and physiological responses of grapevines (*Vitis vinifera* L.) to heat and water stresses under different vineyard cooling and irrigation strategies. *Agronomy*, 11, 1940. https://doi.org/10.3390/agronomy11101940

Collins, C., Gao, H. & Wilkinson, K.L. (2013). An observational study into the recovery of grapevines (*Vitis vinifera* L.) following a bushfire. *American Journal of Enology and Viticulture*, 65(3), 285-292. https://doi:10.5344/ajev.2014.13127

Cunha, M., Marçal, A.R.S. & Silva, L. (2010). Very early prediction of wine yield based on satellite data from vegetation. *International Journal of Remote Sensing*, 31, 3125–3142. https://doi.org/10.1080/01431160903154382

De Bei, R., Fuentes, S., Gilliham, M., Tyerman, S., Edwards, E., Bianchini, N., ... & Collins, C. (2016). VitiCanopy: A free computer App to estimate canopy vigor and porosity for grapevine. *Sensors*, *16*(4), 585. https://doi.org/10.3390/s16040585

De Leeuw, J., Vrieling, A., Shee, A., Atzberger, C., Hadgu, K.M., Biradar, C.M., Keah, H. & Turvey, C. (2014). The potential and uptake of remote sensing in insurance: A review. *Remote Sensing*, 6, 10888–10912. https://doi.org/10.3390/rs61110888

De Vries, C., Buica, A., Brand, J. & McKay, M. (2016). The impact of smoke from vegetation fires on sensory characteristics of Cabernet Sauvignon wines made from affected grapes. *South African Journal of Enology and Viticulture*, 37, 22–30. https://doi.org/10.21548/37-1-755

Devaux, N., Crestey, T., Leroux, C. & Tisseyre, B. (2019). Potential of Sentinel-2 satellite images to monitor vine fields grown at a territorial scale. *OENO One*, 53, 51–58. https://doi.org/10.20870/oeno-one.2019.53.1.2293

Díaz-Delgado, R., Lloret, F. & Pons, X. (2003). Influence of fire severity on plant regeneration by means of remote sensing imagery. *International Journal of Remote Sensing*, 24(8), 1751-1763. https://doi.org/10.1080/01431160210144732

Dutta, R., Das, A. & Aryal, J. (2016). Big data integration shows Australian bushfire frequency is increasing significantly. *Royal Society Open Science*, 3, 150241. https://doi.10.1098/rsos.150241

Edwards E.J., Downie A.F. & Clingeleffer, P.R. (2011). A simple microplate assay to quantify nonstructural carbohydrates of grapevine tissues. *American Journal of Enology and Viticulture*, 62, 133-137. https://doi:10.5344/ajev.2010.10051

Fuentes, S., Tongson, E.J., De Bei, R., Gonzalez Viejo, C., Ristic, R., Tyerman, S. & Wilkinson, K. (2019). Non-invasive tools to detect smoke contamination in grapevine canopies, berries and wine: A remote sensing and machine learning modeling approach. *Sensors*, 19, 3335. https://doi.org/10.3390/s19153335

Giovos, R., Tassopoulos, D., Kalivas, D., Lougkos, N. & Priovolou, A. (2021). Remote sensing vegetation indices in viticulture: A critical review. *Agriculture*, 11, 457. https://doi.org/10.3390/agriculture11050457

Gitelson, A. A., Kaufman, Y. J., Stark, R. & Rundquist, D. (2002). Novel algorithms for remote estimation of vegetation fraction. *Remote Sensing of Environment*, 80(1), 76-87. https://doi.org/10.1016/S0034-4257(01)00289-9

Hamilton, R. (2020). Managing fire affected vineyards. *Australian and New Zealand Grapegrower and Winemaker,* 674, 19-23.

Hantson, S., Arneth, A., Harrison, S.P., & Yue, C. (2016). The status and challenge of global fire modelling. *Biogeosciences,* 13(11), 3359-3375. https://doi:10.5194/bg-13-3359-2016

Hunter K. J. J., Ruffner, H. P. & Volschenk, C. G. (1995). Starch concentrations in grapevine leaves, berries and roots and the effect of canopy management. *South African Journal for Enology and Viticulture*, 16(2), 35-40. https://doi.org/10.21548/16-2-2270

Iland, P., Dry, P., Proffitt, T. & S. Tyerman (2011). *The grapevine: from the science to the practice of growing vines for wine*. (Patrick Iland Wine Promotions, Adelaide).

Jolly, W. M., Cochrane, M., Freeborn, P., Holden, Z.A., Brown, T.J., Williamson, G.J. & Bowman, D. M. J. S. (2015). Climate-induced variations in global wildfire danger from 1979 to 2013. *Nature Communications*, 6, 7537. https://doi.org/10.1038/ncomms8537

Keller, M. & Mills, L.J. (2007). Effect of pruning on recovery and productivity of cold-injured Merlot grapevines. *American Journal of Enology and Viticulture*, 58,351-357.

Kennison, K.R., Wilkinson, K.L., Williams, H.G., Smith, J.H. & Gibberd, M.R. (2007). Smoke-derived taint in wine: Effect of postharvest smoke exposure of grapes on the chemical composition and sensory characteristics of wine. *Journal of Agriculture and Food Chemistry*, 55, 10897–10901. https://doi.org/10.1021/jf072509k

Khaliq, A. Comba, L. Biglia, A. Aimonino, D. R. Y, Chiaberge, M. & Gay, P. (2019). Comparison of satellite and UAV-based multispectral imagery for vineyard variability assessment. *Remote Sensing*, 11, 436. https://doi.org/10.3390/rs11040436

Li, W., Huang, J., Yang, L., Chen, Y., Fang, Y., Jin, H., Sun, H. & Huang, R. (2021). A practical remote sensing monitoring framework for late frost damage in wine grapes using multi-source satellite data. *Remote Sensing*, 13, 3231. https://doi.org/10.3390/rs13163231

Li-Mallet, A., Rabot, A. & Geny, L. (2016). Factors controlling inflorescence primordia formation of grapevine: their role in latent bud fruitfulness? A review. *Botany,* 94, 147-163. https://doi.org/10.1139/cjb-2015-0108

Lopez-Fornieles, E., Brunel, G., Devaux, N., Roger, J. M. & Tisseyre, B. (2022). Is it possible to assess heatwave impact on grapevines at the regional level with time series of satellite images? *Agronomy*, 12(3), 563.

May, P. (2004). *Flowering and fruitset in grapevines*. (Lythrum Press, Adelaide).

Mirabelli-Montan, Y.A., Marangon, M., Graça A., Mayr Marangon, C.M. & Wilkinson, K.L. (2021). Techniques for mitigating the effects of smoke taint while maintaining quality in wine production: A Review. *Molecules*, 26(6), 1672. https://doi.org/10.3390/molecules26061672

Pinel, E.L., Duthoit, S., Costard, A.D., Rousseau, J., Hourdel, J., Vidal-Vigneron, M., Cheret, V. & Clenet, H. (2021). Monitoring vineyard water status using Sentinel-2 images: Qualitative survey on five wine estates in the south of France. *OENO One*, 55, 115–127.

Rawnsley B. & Collins C. (2005). Improving vineyard productivity through assessment of bud fruitfulness and bud necrosis. Final report to the Grape and Wine Research and Development Corporation – SAR 02/05, Adelaide, Australia. https://www.wineaustralia.com/getmedia/1b8f407d-6891-4971-bb57-4c7bc2c532ef/SAR-02-05

Ristic, R., Osidacz, P., Pinchbeck, K., Hayasaka, Y., Fudge, A. & Wilkinson, K. (2011). The effect of winemaking techniques on the intensity of smoke taint in wine. *Australian Journal of Grape and Wine Research*, 17, 29–40. https://doi.org/10.1111/j.1755-0238.2011.00146.x

Ristic, R., Fudge, A.L., Pinchbeck, K.A., De Bei, R., Fuentes, S., Hayasaka, Y., Tyerman, S.D. & Wilkinson, K.L. (2016). Impact of grapevine exposure to smoke on vine physiology and the composition and sensory properties of wine. *Theoretical and Experimental Plant Physiology*, 28, 67–83. https://doi.org/10.1007/s40626-016-0054-x

Rose, B. (2009). Pruning smoke, fire and heat-impacted vines. *Australian and New Zealand Grapegrower and Winemaker,* 545, 34–35.

Scarlett, N., Needs, S. & Downey, M.O. (2011). Assessing vineyard viability after bushfire. *Australian and New Zealand Grapegrower and Winemaker*, 564, 21-25.

van der Hulst, L., Munguia, P., Culbert, J.A., Ford, C.M., Burton, R.A. & Wilkinson, K.L. (2019). Accumulation of volatile phenol glycoconjugates in grapes following grapevine exposure to smoke and potential mitigation of smoke taint by foliar application of kaolin. *Planta*, 249, 941–952. https://doi.org/10.1007/s00425-018-03079-x

Wang, X., De Bei, R., Fuentes, S. & Collins, C. (2019). Influence of canopy management practices on canopy architecture and reproductive performance of Semillon and Shiraz grapevines in a hot climate. *American Journal of Enology and Viticulture*, *70*(4), 360-372. https://doi.org/10.5344/ajev.2019.19007

Westerling, A. L., Hidalgo, H. G., Craven, D. R. and Swetnam, T. W. (2006). Warming and earlier spring increase Western U.S. forest wildfire activity. *Science*, 313, 940–943. https://doi.org/10.1126/science.1128834

Westerling, A. L. (2016). Increasing western US forest wildfire activity: sensitivity to changes in the timing of spring. *Philosophical Transactions of the Royal Society B,* 371, 20150178. https://doi.org/10.1098/rstb.2015.0178

Whiting, J. (2012). Recovery of grapevines from fire damage. *Australian and New Zealand Grapegrower and Winemaker,* 580, 25-31.

Wilkinson, K. & Collins, C. (2010). Grapevine recovery following fire damage. *Australian and New Zealand Grapegrower and Winemaker,* 556, 42-43.

Wilkinson, K.L., Ristic, R., Pinchbeck, K.A., Fudge, A.L., Singh, D.P., Pitt, K.M., Downey, M.O., Baldock, G.A., Hayasaka, Y., Parker, M. & Herderich, M.J. (2011). Comparison of methods for the analysis of smoke related phenols and their conjugates in grapes and wine. *Australian Journal of Grape Wine Research*, 17, 22–28. https://doi.org/10.1111/j.1755-0238.2011.00147.x

Winkler, A. J. & Williams, W. O. (1945). Starch and sugars of *Vitis vinifera*. *Plant Physiology*, 20(3), 412-432. https://doi.org/10.1104/pp.20.3.412

Wolfe, W. (2001). Vine and management following low temperature injury. In: Proceedings of the ASEV 50th Anniversary Annual Meeting. J.M. Rantz (ed.), pp. 101-110. American Society for Enology and Viticulture, Davis.

Xue, J. & Su, B. (2017). Significant remote sensing vegetation indices: A review of developments and applications, Journal of Sensors, 2017, 1353691. https://doi.org/10.1155/2017/1353691

12. Appendix 4: Staff

The following people were engaged on the Project:

University of Adelaide
A/Prof Cassandra Collins
Dr Roberta De Bei
Mrs Annette James
Mr Lucas De Simoni
Mr Patrick O'Brien

Consilium Technology
Dr Michaela Ritchie
Dr Saisai Ma
Mr Andy Clarke
Dr Sebastien Wong
Dr Jingyun Ouyang